IDENTIFICATION OF MEMORY TERMS IN A POWER AMPLIFIER

A THESIS SUBMITTED TO
THE GRADUATE SCHOOL OF NATURAL AND APPLIED SCIENCES
OF
MIDDLE EAST TECHNICAL UNIVERSITY

BY

ERHAN DURSUN

IN PARTIAL FULLFILLMENT OF THE REQUIREMENTS
FOR
THE DEGREE OF MASTER OF SCIENCE
IN
ELECTRICAL AND ELECTRONICS ENGINEERING

DECEMBER 2013

Approval of the thesis:

IDENTIFICATION OF MEMORY TERMS IN A POWER AMPLIFIER

submitted by **ERHAN DURSUN** in partial fulfillment of the requirements for the degree of **Master of Science in Electrical and Electronics Engineering Department, Middle East Technical University** by,

Prof. Dr. Canan Özgen
Dean, Graduate School of **Natural and Applied Sciences** _____

Prof. Dr. Gönül Turhan Sayan
Head of Department, **Electrical and Electronics Eng.** _____

Prof. Dr. Şimşek Demir
Supervisor, **Electrical and Electronics Eng. Dept., METU** _____

Examining Committee Members:

Prof. Dr. Canan Toker
Electrical and Electronics Eng. Dept., METU _____

Prof. Dr. Şimşek Demir
Electrical and Electronics Eng. Dept., METU _____

Prof. Dr. Gönül Turhan Sayan
Electrical and Electronics Eng. Dept., METU _____

Asst. Prof. Dr. Ahmet Hayrettin Yüzer
Electrical and Electronics Eng. Dept., KBU _____

Bülent Şen, M.Sc.
Senior Lead Design Engineer, ASELSAN _____

Date: 09.12.2013

I hereby declare that all information in this document has been obtained and presented in accordance with academic rules and ethical conduct. I also declare that, as required by these rules and conduct, I have fully cited and referenced all material and results that are not original to this work.

Name, Last name : Erhan DURSUN

Signature :

ABSTRACT

IDENTIFICATION OF MEMORY TERMS IN A POWER AMPLIFIER

Dursun, Erhan
M. Sc., Department of Electrical and Electronics Engineering
Supervisor: Prof. Dr. Şimşek Demir
December 2013, 98 pages

Behavioral models are valuable tools which bring ability to simulate a device without knowing inside of the device. Behavioral modeling is functional in many areas. Power amplifier which is a crucial device for RF/Microwave systems is also an application area of behavioral modeling. Static Nonlinearity -AM/AM, AM/PM distortion- and Dynamic Nonlinearity –memory effect- are issues of power amplifier behavioral modeling.

Memory effect is an undesired behavior seen in power amplifiers. Memory means output produced is not only determined by present input but also by previous inputs. Bandwidth of input signal, input power level, bias circuit components and semi-conductor characteristics are some sort of factors affecting memory.

In this thesis, a behavioral model that exhibits memory effect is proposed. Model is constructed for a 1-2 GHz 10W output power (in saturation) class AB power amplifier. Approach applied is compared with previous modeling approaches and advantages of proposed model are presented. Additionally, relation between bias circuit components and memory is investigated.

Keywords: Power Amplifier, Memory Effect, Modeling, Linearity.

ÖZ

BİR GÜÇ YÜKSELTECİN HAFIZA TERİMLERİNİN BELİRLENMESİ

Dursun, Erhan
Yüksek Lisans, Elektrik ve Elektronik Mühendisliği Bölümü
Tez Yöneticisi: Prof. Dr. Şimşek Demir
Aralık 2013, 98 sayfa

Davranışsal modeller bir donanımın iç yapısını bilmeksizin o donanımın davranışlarını sergileme becerisi getiren yararlı araçlardır. Davranışsal modelleme pek çok alanda kullanılmaktadır. RF/Mikrodalga sistemler için kritik bir donanım olan güç yükselteç de davranışsal modellemenin bir uygulama alanıdır. Statik doğrusal olmama -AM/AM, AM/PM bozulması- ve dinamik doğrusal olmama – hafıza etkisi- güç yükseltecin davranışsal modellemesinin konularıdır.

Hafıza etkisi güç yükselteçlerde görülen istenmeyen bir davranıştır. Hafıza, güç yükseltecin çıkışının o anda yükselteci uyaran giriş işaretine bağlı olmayıp daha önce yükselteci uyaran giriş işaretlerine de bağlı olması durumudur. Giriş işaretinin bant genişliği, giriş işaretinin seviyesi, ön gerilimleme devresindeki elemanlar ve yarı-iletkenin karakteristiği hafızayı etkileyen bir takım etkenlerdir.

Bu tez çalışmasında, hafıza etkisi sergileyen bir davranışsal model önerilmektedir. Model 1-2 GHz frekans bandında çalışan, 10W çıkış gücüne sahip (doyumda) AB sınıfı bir güç yükselteç için oluşturulmuştur. Uygulanan yöntem önceki modelleme uygulamaları ile kıyaslanmış ve önerilen modelin avantajları sunulmuştur. Ayrıca, ön gerilimleme devresi elemanları ile hafıza arasındaki ilişki araştırılmıştır.

Anahtar Kelimeler: Güç Yükselteç, Hafıza Etkisi, Modelleme, Doğrusallık.

To My Nieces,

ACKNOWLEDGEMENTS

I would like to express my special appreciation and thanks to my advisor Prof. Dr. Şimşek DEMİR, you have been a tremendous mentor for me. I would like to thank you for encouraging my research and for supporting me to improve my capability as a researcher. Your advices on research have been priceless. I would also like to thank my committee members, Prof. Dr. Canan TOKER, Prof. Dr. Gönül Turhan SAYAN, Asst. Prof. Dr. Ahmet Hayrettin YÜZER, Senior Lead Design Engineer Bülent ŞEN for serving as my committee members. I also want to thank you for letting my defense be an enjoyable moment and for your brilliant comments and suggestions, thanks to you.

A special thanks to my family. Words cannot express how grateful I am to my mother, father, sister, brother-in-law for all the sacrifices that you've made on my behalf. Your prayer for me was what sustained me thus far. I would also like to thank my friends Mustafa DURUKAL, Selçuk ÖKSÜZ who supported me in writing and encouraged me to strive towards my goal.

TABLE OF CONTENTS

LIST OF TABLES

LIST OF FIGURES

LIST OF ABBREVIATIONS

ACPR	: Adjacent Channel Power Ratio
CDMA	: Code Division Multiple Access
DPD	: Digital Predistortion
DSP	: Digital Signal Processing
EER	: Envelope Elimination and Restoration
FFT	: Fast Fourier Transform
FM	: Frequency Modulation
IMD	: Intermodulation Distortion
OFDM	: Orthogonal Frequency Division Multiplexing
OIP_3	: Output Third Order Intercept Point
PA	: Power Amplifier
QAM	: Quadrature Amplitude Modulation
RF	: Radio Frequency

CHAPTER 1

INTRODUCTION

1.1 Foreword

Power amplifier is a significant device for wireless communication systems. A PA boosts RF signal power to transmit through the air medium. It is generally the most energy consuming part of the system. Therefore, efficiency is a concern for PA designers. Efficiency is the ratio of RF power and drawn dc power.

$$Efficiency = \frac{P_{RF}}{P_{DC}} \tag{1.1}$$

A PA has tendency to work inefficient in linear region where the gain of the amplifier stays stable. However, PA works with high efficiency in saturation region where nonlinear behavior dominates. There is a trade-off between linearity and efficiency.

The main source of nonlinearity in wireless communication systems is PA. PAs used for communication applications have to work with high linearity because nonlinearity brings distortion in amplitude and phase. Modulation types such OFDM and QAM used for high spectral efficiency bring the necessity of linearity [1]. Intermodulation products and harmonics occur at the output of amplifier because of nonlinearity. Harmonic filter is used to get rid of harmonics but it is not easy to be rescued from frequency components occur in band. Therefore, linearization methods are used. Some sort of linearization methods are Predistortion, Feedback and Feedforward structures. These methods bring opportunity to satisfy linearity and efficiency.

One of the most popular linearization techniques is predistortion. Relation between input and output of the amplifier is required to apply predistortion. In predistortion, signal is distorted as a complement of input-output function of the PA; this cancels distortion effect and linearity is satisfied.

Behavioral Modeling is significant for identifying relation between input and output of the amplifier. Modeling nonlinearity of PA is the first step of analyzing a PA and designing a linearizer for PA [2]. Behavioral modeling is generally preferred to model PAs because it brings a relation between input and output without spending time for a physical analysis. The method which is followed while gathering a behavioral model has distinct steps. Nonlinear behavior of PA is measured first; then parameters of a predefined model are extracted. A measurement set up which brings magnitude and phase of frequency components is essential for nonlinearity measurements.

Nonlinearity which is seen in PAs is divided into two; Static Nonlinearity and Dynamic Nonlinearity. Static Nonlinearity is described with AM/AM and AM/PM curves. Static Nonlinearity is modeled with inputs achieved from AM/AM and AM/PM measurements. It is seen that asymmetry between lower and upper sidebands varies depending on the bandwidth of input signal which means that AM/AM and AM/PM curves are dynamic. This is called memory effect [2].

In Dynamic Nonlinearity, distortion of amplifier changes with bandwidth of input signal. Also electro-thermal characteristic of the semi-conductor, bias circuit components and input power level affect distortion of PA. Dynamic Nonlinearity which is named as “memory effect” means output of amplifier is not only determined by present input but also by previous inputs. Thermal effects and long time constants arising from bias circuit components are causes of memory effect that is seen in PAs [2].

This thesis mainly focuses on modeling of a 1-2 GHz 10W output power (in saturation) class AB PA. A polynomial which describes input-output relation of PA is proposed and parameters of the polynomial are investigated. Polynomial contains delay terms which simulate memory behavior. Delay terms are achieved

by using a unique methodology and memory of PA is identified. Also, the relation between delay terms and bias circuit components are investigated.

1.2 Objectives

Objectives of this thesis are;

- to have knowledge about PA nonlinearity and memory effect,
- to construct a behavioral model for a 1-2 GHz 10W output power class AB power amplifier,
- to identify causes of memory effect,
- to discover effect of bias circuits components on delay terms.

1.3 Outline

Outline of the thesis is as follows;

In second chapter, fundamentals of behavioral modeling are reviewed. Importance of PA modeling is explained and some types of behavioral modeling are discussed. Linearization is an issue in this chapter; necessity of linearization and linearization methods are mentioned. Memory effect is a subtitle in the second chapter; basics of memory effect, factors that create memory and types of memory are discussed.

Memory model is the focus of third chapter. Model polynomial is introduced in this chapter and model construction methodology is described in detail. Measurement infrastructure built for modeling purpose is presented.

In fourth chapter performed measurements are described; results and extracted model polynomial parameters are presented. Validity of the model is examined. Effect of bias circuit components on delay terms is investigated and results are presented with comparison.

In last chapter, results are examined; conclusions of the thesis and future work to enhance proposed model are explained.

CHAPTER 2

BEHAVIORAL MODELING

FM signal which is a kind of RF signal was used in the previous communication systems. PAs that work with high efficiency are possible in those systems because information is not stored on amplitude of RF signal. Presently, requirements and technology are not same; new modulation schemes which promise capacity improvements are used.

Wireless communication systems are under pressure of providing service to more users and the demand on high data rates increases day by day. Modulation schemes such CDMA and OFDM which have ability to carry high data rates are used to meet requirements. However, these schemes have amplitude modulated envelope and any nonlinear behavior seen in PA causes emission of transmitted signal over spectrum. Spreading causes interference with neighboring channels so spacing is required between transmission channels to avoid interference. But, this is an inefficient usage of frequency spectrum and not a rational method.

If a PA works in saturation region then it produces nonlinearity. Working in this region is essential to satisfy output power requirement and also provides higher efficiency.

To improve efficiency and linearity, different PA structures and different methodologies are used. For example, Doherty type amplifiers are used not to lose efficiency while working at back off. And to improve linearity, linearization methods such digital predistortion are used. DPD is the most preferred method for signals which have MHz level bandwidth. DPD needs to know nonlinear behavior of PA to

produce an inverse function and to cancel nonlinearity. Thus, behavioral modeling is important for producing inputs to DPD. The best part of behavioral modeling is the fact that users don't need to know the inside of RF circuit and interaction of circuit components with each other; the only important thing is to know the mathematical expression which relates input signal to output signal [3]. This type of modeling approaches brings system engineers opportunity to simulate whole system and engineers who work on linearization to study with information close to real. There are critical features to take care when modeling a PA.

- Producing proper signals at the input and output of the amplifier. Generating the behavior which is tried to be modeled.
- Achieving a formula which models all important interaction between input and output signals [3].

Generally AM-AM and AM-PM curves are the main instruments that are used to model PA nonlinearity. However, increase of the bandwidth of input signal creates dispersion effect on these curves and this makes modeling difficult. Figure 2-1 shows the effect of memory on input power/output power graph and input power/output phase graph. Significant dispersion effect is seen on the graphs.

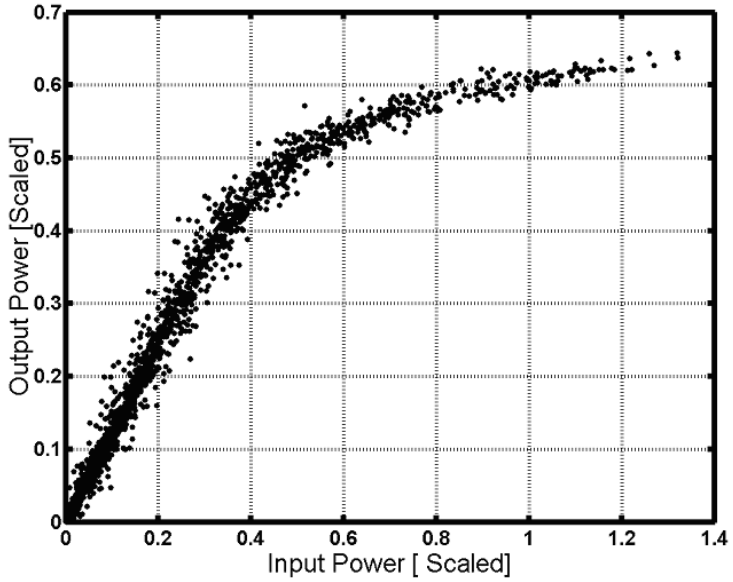

(a)

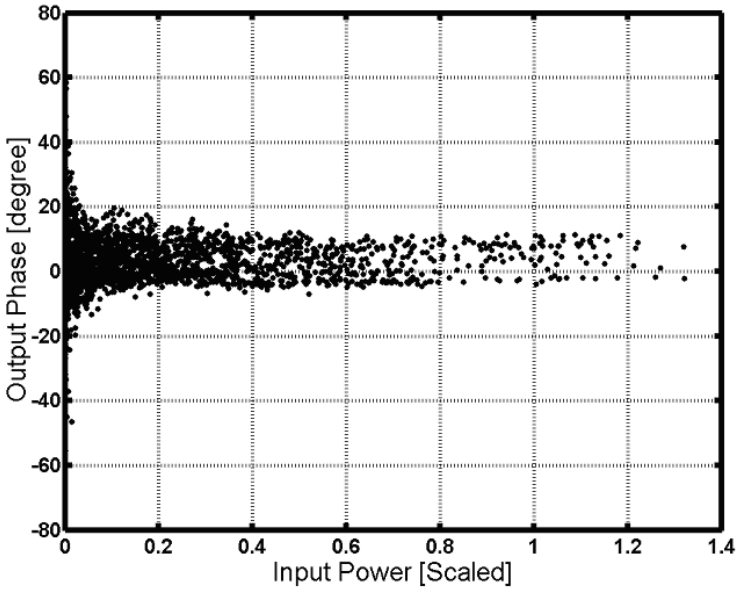

(b)

Figure 2-1 AM-AM and AM-PM response of a LDMOS PA (a) Input Power vs. Output Power (b) Input Power vs. Output Phase [2]

In [5], it is stated that PA models can be grouped into two: physical models and empirical models.

Components in the circuit, relation between them and analytical rules defining their interaction are concerns of physical modeling. Physical models use nonlinear model

of active device and passive components around active device to build nonlinear equations which relate voltages and currents at the terminals. This type of models is convenient for circuit level simulation. Active device nonlinear model is the significant factor that limits the accuracy. This type of models causes long simulation time and requires comprehensive knowledge about PA circuit [5].

Empirical models use data which is achieved from measurements to create a model. The data is fitted to a predetermined model and model parameters are identified. This process is a kind of curve fitting.

PA behavioral models are helpful if system level simulation is desired. Behavioral model strongly depends on parameter extraction method, predefined model structure and data achieved from measurements. Different data sets which are used for model construction produce different models. Thus, great care must be devoted to the measurements. It should also be known that behavioral models are application specific; it is not always possible to use a behavioral model in all cases or conditions.

There are different types of behavioral models. Types of behavioral models and properties of these models are listed in the figure below:

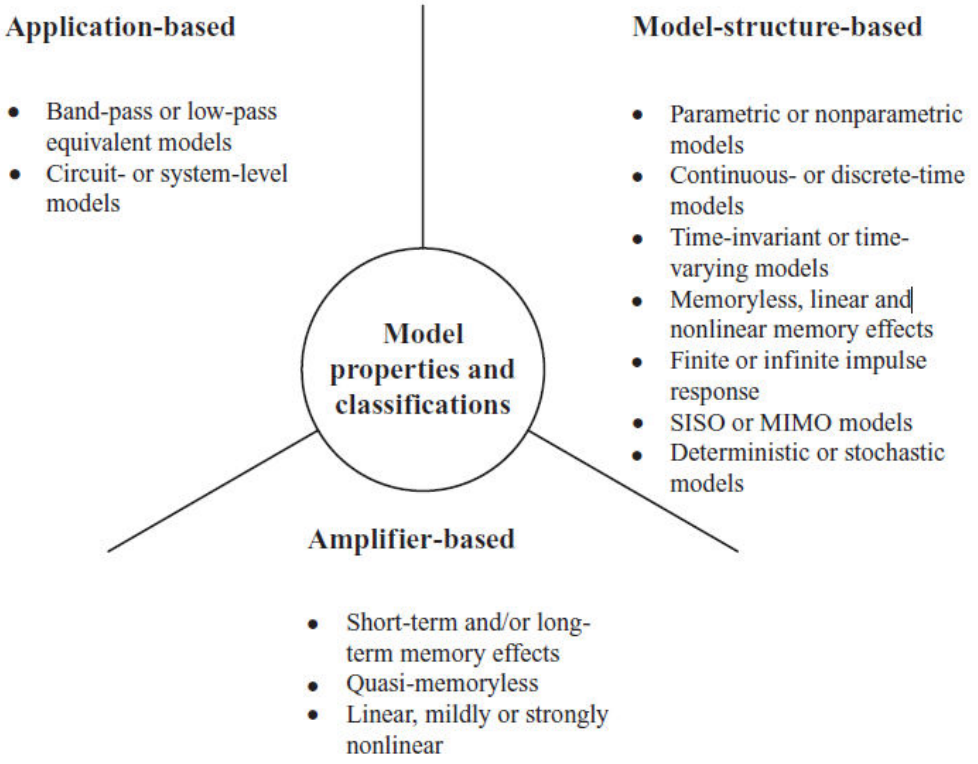

Figure 2-2 Behavioral Model Types and Properties of These Models [6]

In Figure 2-2, behavioral models are categorized into three main groups: Application-based, Model-structure-based and Amplifier-based. It is known that there are different methods of extracting a relation between input and output of a PA.

Mathematical modeling and system identification are types of methods used to assemble a model. Mathematical modeling uses a theoretical expression to relate input to output and investigates parameters of the expression. Despite, in system identification method convenient model parameters are investigated which fits achieved data to the measurements. Behavior of cascaded structure like multistage amplifier is more complex; it is not easy to present a theoretical expression. Hence, it is more useful to use system identification method.

The properties of models which are produced by system identification method are:

- They are valid or useful for some certain conditions (not for all working modes of PA)
- No huge knowledge is required to construct

- It is simple to construct

Behavioral modeling wholly depends on the data which is achieved from measurements. Thus, to construct a fine model which represents all conditions of PA, it is essential to excite all working modes of PA and to collect data carefully. It is important to decide a transfer function which has appropriate number of coefficients or unknowns for simulating PA behavior. Otherwise, unnecessary coefficients increase complexity of parameter extraction process and may be it wouldn't be possible to identify every parameter of the model.

While performing measurements choosing the excitation signal is crucial. A two tone signal creates intermodulation products and harmonics at the output of PA when working in nonlinear regime. Amplitude and phase of frequency components which arise at the output furnish equations to identify the unknowns of the transfer function. Moreover, a two tone signal is suitable because it is easy to produce and has a non-constant envelope. This signal type brings opportunity of achieving important information such intercept points [6]. Two tone measurements which are performed with different tone spacings and different input power levels prove existence of memory effects.

2.1 Memory Effect

In the previous sections, memory effect is determined and shortly mentioned. In this section memory effect is discussed in detail.

Different classifications of memory effects exist in literature; one of the classifications groups memory effects as Linear Memory and Nonlinear Memory. According to another point of view, memory effects are classified as Short Term Memory Effects and Long Term Memory Effects. Equivalent circuit model description of a transistor causes this classification.

Capacitors and inductors (components storing charge and magnetic flux) don't exist in a memoryless circuit. Thus, voltages and currents on terminals of the circuit don't depend on the previous voltages and currents. In a power amplifier circuit, capacitors and inductors exist in matching network and bias network. Also, equivalent circuit

model of a transistor includes capacitors and inductors. In some applications, it is possible to neglect memory effects because ratio between center operation frequency and information bandwidth is very high which renders possible to disregard frequency dependent behaviors [6]. Input and output matching networks have band-pass characteristics and transistor itself shows low-pass characteristics. These behaviors contribute to the short-term memory. Figure below summarizes the idea.

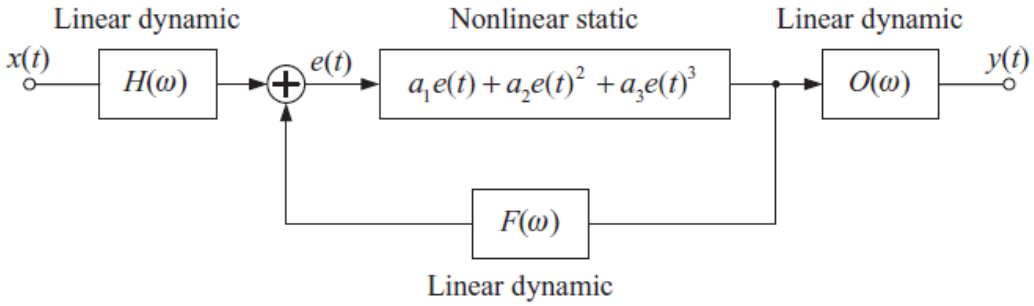

Figure 2-3 Nonlinear Feedback Structure of a PA [6]

Filters H(ω) and O(ω) which are shown in Figure 2-3 represent linear memory effects that are caused by input and output matching networks respectively. Nonlinear memory effects that are caused by electro-thermal coupling and bias circuit is represented with a feedback structure, F(ω).

Long term memory effects are more complex than short term memory effects. There are many reasons causing long term memory such: trapping effect, self heating, input-output bias circuit and envelope feedback loops.

An envelope feedback loop can occur if a proper isolation isn't provided between input and output bias circuits. This can also occur if voltages of gate and drain are supplied from same device.

Dissipated power of a transistor depends on threshold voltage, drain current, temperature dependent carrier mobility and carrier saturation velocity [6]. Dissipated power change causes temperature change and self heating. Because of the physics of the transistor, self heating of the amplifier is frequency dependent. This mechanism shows low frequency feedback characteristics hence creates long term memory.

Trapping is another cause of long term memory effects seen in PAs. If envelope components occur at the drain of transistor move back to the gate of transistor this is called trapping effect. A remixing event occurs between envelope components and RF components and a low frequency feedback condition arises. It can be said that structures defining drain or base low frequency impedance change are main factors of long term memory generation.

Usual memoryless predistortion linearizers are not able to suppress out of band emission which is originated from memory effects [7]. It is possible to observe spectrum regrowth originated from memory effects by applying memoryless predistortion to the PA. Memoryless predistortion eliminates Static Nonlinearity and only Dynamic Nonlinearity, which is at the same time called memory effect, remains. Thus, while observing spectrum only out of band emission caused by memory effects is seen. Figure below illustrates the approach.

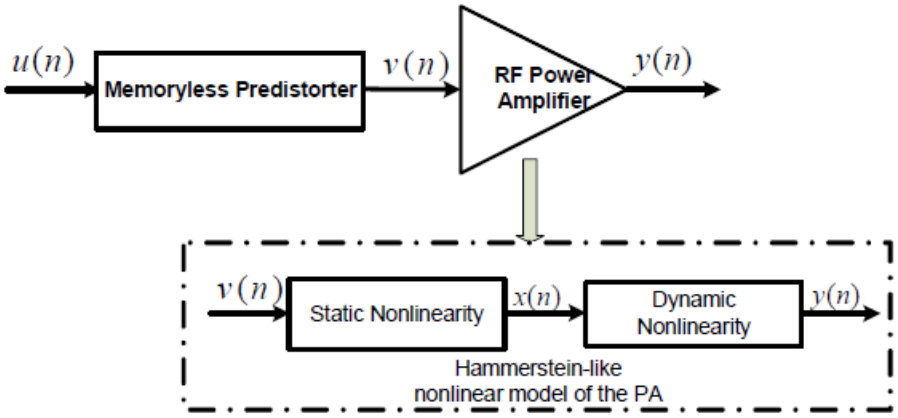

Figure 2-4 Method for Decomposing Out of Band Emission Caused by Memory Effects [1]

It is known that increase of input power strengthens memory effects. Thus, high input power causes higher out of band emission.

There are types of methods in literature for PA modeling. In this thesis study, the author is interested in behavioral models exhibiting memory. Volterra series is a well known model exhibiting memory but it has high complexity; so modelers do not prefer nowadays. Wiener and Hammerstein are other model types; according to

Volterra series these models are easier. Recently, memory polynomial model is the most conspicuous model type because of its simplicity [8]. In [8], three different memory polynomial models are described. In consequent section, these models will be summarized. First of them is memory polynomial model.

2.1.1 Memory Polynomial Model

Memory polynomial model is also known as augmented nonlinear moving average model. This model describes both nonlinearity and memory. Figure illustrating memory polynomial model is seen below.

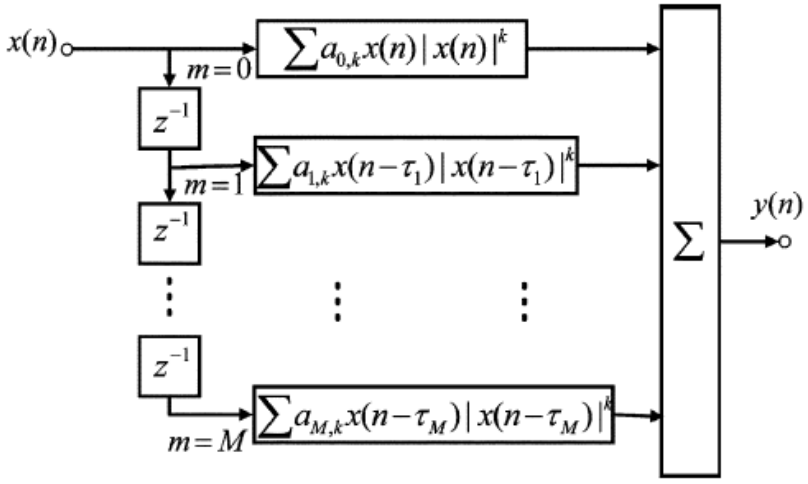

Figure 2-5 Architecture of Memory Polynomial Model [8]

Input output relation is written as follows:

$$y(n) = \sum_{m=0}^{M} \sum_{k=0}^{K} a_{m,k} x(n-\tau_m) \left| x(n-\tau_m) \right|^k \qquad (2.1)$$

x(n) and y(n) are the complex envelope input and output signals. $a_{m,k}$ represent coefficients of the model. k defines order of nonlinearity and m defines memory depth. Delay term is defined as $\tau_m = \tau_0 . m$ where τ_0 is the sampling time interval of the input signal. Memory depth and order of nonlinearity can be altered for accuracy but this brings complexity and causes difficulty while extracting model parameters.

2.1.2 Non-Uniform Delay Memory Polynomial Model

The input-output relation of non-uniform delay memory polynomial model is similar to the memory polynomial model. The differences are number of delay terms and calculation of delay terms.

$$y(n) = \sum_{l=0}^{L} \sum_{k=0}^{K} a_{l,k} x(n-\tau_l) \left| x(n-\tau_l) \right|^k \tag{2.2}$$

Input-output relation of non-uniform delay memory polynomial is seen above. Calculation of τ_l and L is different and difficult than the calculation of τ_m and M. In this model type, a method is proposed to identify the delay term τ_l. The outputs of different delays are assumed to be irrelevant; thus describing τ_1 most important delay term is possible by using cross correlation of input signal and polynomial model error. A noteworthy peak seen in cross correlation can be evidence of a significant delay in output signal. Algorithms can be used to converge exact value of τ_1. Normalized Mean Square Error is a kind of criterion which can be used for this purpose.

$$NMSE = 10 \log \frac{\sum_{i=1}^{N} \left| y(i) - y(i)_{model} \right|^2}{\sum_{i=1}^{N} \left| y(i) \right|^2} \tag{2.3}$$

Formulation to calculate NMSE is seen in equation (2.3). $y(i)$ is output of PA, $y(i)_{model}$ is the output of proposed model. NMSE criterion is also convenient for verification of proposed models.

2.1.3 Enhanced Memory Polynomial Model

Memory polynomial is not successful on defining strong nonlinear memory effects. Thus, to exhibit nonlinear memory, products of first order delayed samples of input and memory polynomials of current samples are added to the memory polynomial

model [8]. The new generated model is called Enhanced Memory Polynomial Model. Figure below illustrates the model.

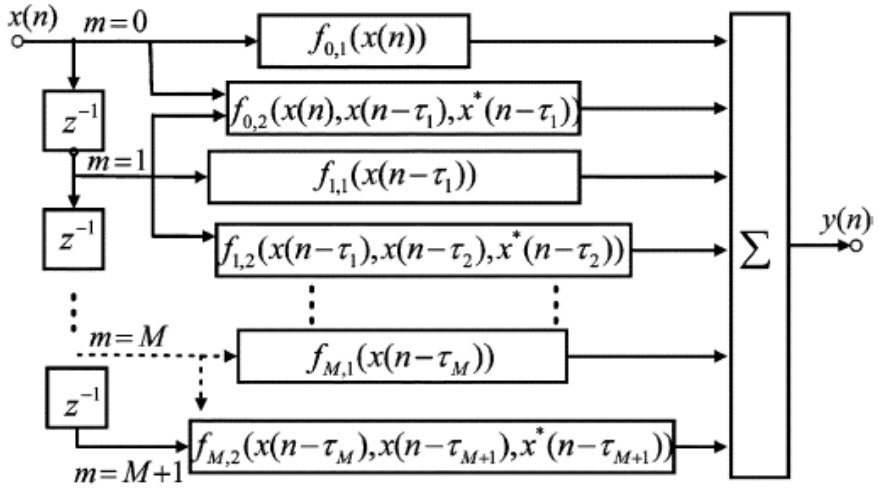

Figure 2-6 Architecture of Enhanced Memory Polynomial Model [8]

The equation seen below determines the input-output relation of enhanced memory polynomial model;

$$y(n)=\sum_{m=0}^{M}\left\{\begin{array}{l} x(n-\tau_m)\sum_{k=0}^{K}a_{m,k}^{1}\left|x(n-\tau_m)\right|^{k} \\ +x(n-\tau_m-\tau_0)\sum_{k=0}^{K}a_{m,k}^{2}\left|x(n-\tau_m)\right|^{k} \\ +x^{*}(n-\tau_m-\tau_0)x(n-\tau_m)^{2} \\ x\sum_{k=0}^{K}a_{m,k}^{3}\left|x(n-\tau_m)\right|^{k} \end{array}\right\} \tag{2.4}$$

$a_{m,k}^{i}\quad i=1,2,3$ is coefficient of the model. Enhanced memory polynomial model includes three different components. One of them is identical with memory polynomial. Second and third components are nonlinear function of neighboring sample points and they describe the nonlinear memory effect of the sample PA.

In [8], it is reported that non uniform delays reduce complexity and usage of nonlinear model improves accuracy.

2.2 Types of Memory Effect

Generally, memory effects are grouped into two: Thermal Memory Effect and Electrical Memory Effect. Thermal Memory is a long term memory; it is effective when excitation signal bandwidth is narrow. Envelope period of a narrow band excitation signal is long thus, envelope amplitude varies slowly. When envelope amplitude increases dissipated power also increases; this condition triggers thermal memory sources.

Electrical memory is a short term memory. It is effective when excitation signal bandwidth is wide for example 10 or 20 MHz. Envelope period is short and envelope of wideband signal varies rapidly. Matching network, charge storing and magnetic flux storing components are causes of electrical memory.

It is known that amplitude and phase of IM3 components vary asymmetrically depending on input power level and excitation signal bandwidth. 0.5 dB amplitude increase or 10-20° phase rotation of an IM3 component depending on tone spacing increase is not tragic when performing two-tone test. Especially, ACPR which is basically described as power leakage to the adjacent channels is not affected dramatically from such condition [9].

2.3 Linearization

An easy way of linearizing class-A type amplifier is operating at back-off. When output power is reduced from its highest value, distortion products are gone. However, this approach reduces efficiency dramatically. Figure below illustrates efficiency as a function of IM3 level.

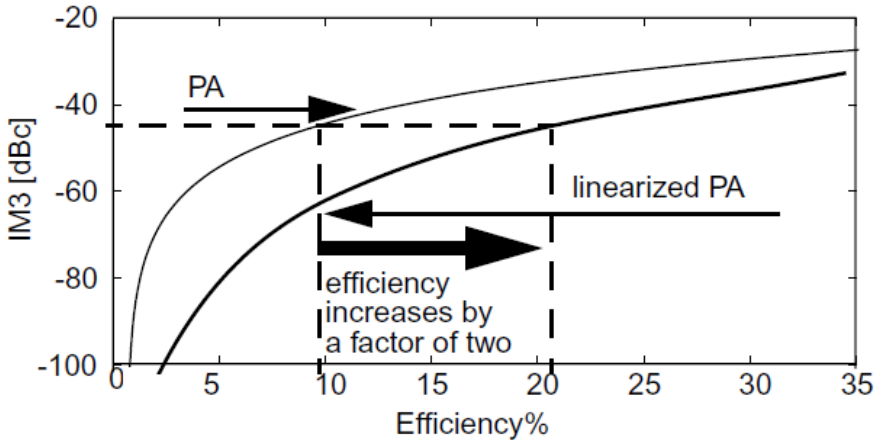

Figure 2-7 Efficiency comparison of linearized PA and PA working at back-off [9]

Linearization methods also consume energy but this energy is less than the energy acquired from efficiency improvement. The general approach is to design an efficient PA then apply a linearization method to satisfy linearity because efficiency is determined by PA and linearity is determined by linearization method.

Feedback, Feedforward, DPD, Envelope Elimination and Restoration are types of linearization methods. In the next part, DPD method which is related to memory effect is discussed.

2.3.1 Digital Predistortion

Predistortion is one of the most popular linearization methods and may be it is the easiest for implementation. General idea is applying a complementary distortion prior to PA. Distortion of PA and complementary distortion of predistorter eliminate each other; thereby linearization is maintained. Two different methods exist; one of them is digital, other one is transfer characteristic method [10]. In the first method, digital signal processing is used to implement predistortion. It is possible to apply DSP at any instance; but the cheapest choice is applying at the baseband. First, knowledge to implement predistortion is described and stored in memory then stored information is used to predistort signal. In the second method, transfer characteristic of the PA is determined and a hardware which produces such characteristic is implemented. Implementing such hardware can be more difficult than using DSP method. Success of these methods is limited by the ability of producing desired predistortion effect.

In the previous paragraph, it is stated that predistortion methods are divided into two groups; digital predistortion and transfer characteristic method. Whereas, there is one other kind exists; Adaptive Predistortion. In this type, a feedback mechanism exists; this structure determines an error function. DSP algorithms are used to minimize error function continuously. Correction is carried out while operation is running thus, better predistortion is realized. However, method has disadvantages: DSP algorithms should run rapidly, also structure should be talented to compensate delays resulting from feedback.

CHAPTER 3

MEMORY MODEL

3.1 Model Polynomial

In this chapter, theoretical background of a memory model which is proposed in [11] is investigated. Model describes a relation between time domain input signal and time domain output signal of a PA. It has ability to determine both, nonlinearity and memory. Model includes third and fifth order terms. Unequal delay terms are located to exhibit memory. In the continuing sections of this chapter, proposed method which is used to identify unequal delay terms is described.

A power amplifier is a non-linear device and its transfer function can be written as;

$$V_0(t) = a_1 V_i(t) + a_3 V_i^3(t) + a_5 V_i^5(t) + ... + a_n V_i^n(t) \quad (3.1)$$

Even order terms are removed because a general hypothesis dictates that they don't have any contribution to intermodulation terms. It is predicted that a 5^{th} order polynomial is enough to simulate nonlinear behavior of the PA which is going to be modeled. Polynomial given below is the core expression which determines input signal – output signal relation;

$$V_o(t) = a_1 V_i(t - \tau_1) + a_3 V_i^3(t - \tau_3) + a_5 V_i^5(t - \tau_5) \quad (3.2)$$

a_1, a_3 and a_5 are coefficients of the polynomial; τ_1, τ_3 and τ_5 are unequal delay terms that are used to exhibit memory.

While measuring PA characteristics, excitation signal is significant. Memory model together with excitation signal produce adequate number of equations to extract model parameters. A two-tone signal which produces intermodulation products and harmonics at the output of PA is suitable for this process.

A two tone signal is written as;

$$V_i(t) = A_1 Cos(\omega_1 t) + A_2 Cos(\omega_2 t + \varphi) \tag{3.3}$$

If equation (3.2) is rewritten using equation (3.3), equation (3.4) is achieved.

$$\begin{aligned} V_o(t) = a_1[A_1 Cos(\omega_1(t-\tau_1)) + A_2 Cos(\omega_2(t-\tau_1)+\varphi)] + a_3[A_1 Cos(\omega_1(t-\tau_3)) \\ + A_2 Cos(\omega_2(t-\tau_3)+\varphi)]^3 + a_5[A_1 Cos(\omega_1(t-\tau_5)) + A_2 Cos(\omega_2(t-\tau_5)+\varphi)]^5 \end{aligned} \tag{3.4}$$

To observe the frequency components occurred at the output of PA, equation (3.4) is expanded and written as sum of Cosines.

$$\begin{aligned} V_o(t) = a_1\left[A_1 Cos(\omega_1(t-\tau_1)) + A_2 Cos(\omega_2(t-\tau_1)+\varphi)\right] + a_3[{3A_1^3}/{4}\, Cos(\omega_1(t-\tau_3)) \\ + {A_1^3}/{4}\, Cos(3\omega_1(t-\tau_3)) + {3A_1^2A_2}/{2}\, Cos(\omega_2(t-\tau_3)+\varphi) \\ + {3A_1^2A_2}/{4}\, Cos((2\omega_1+\omega_2)(t-\tau_3)+\varphi) + {3A_1^2A_2}/{4}\, Cos((2\omega_1-\omega_2)(t-\tau_3)-\varphi) \\ + {3A_1A_2^2}/{2}\, Cos(\omega_1(t-\tau_3)) + {3A_1A_2^2}/{4}\, Cos((2\omega_2+\omega_1)(t-\tau_3)+2\varphi) \\ + {3A_1A_2^2}/{4}\, Cos((2\omega_2-\omega_1)(t-\tau_3)+2\varphi) + {3A_2^3}/{4}\, Cos(\omega_2(t-\tau_3)+\varphi) \\ + {A_2^3}/{4}\, Cos(3\omega_2(t-\tau_3)+3\varphi)] \end{aligned}$$

$$
\begin{aligned}
&+a_5[\,{}^{5A_1^5}\!/_{8}\,Cos\left(\omega_1(t-\tau_5)\right)+{}^{5A_1^5}\!/_{16}\,Cos\left(3\omega_1(t-\tau_5)\right)\\
&+{}^{A_1^5}\!/_{16}\,Cos\left(5\omega_1(t-\tau_5)\right)+{}^{15A_1^4A_2}\!/_{8}\,Cos\left(\omega_2(t-\tau_5)+\varphi\right)\\
&+{}^{5A_1^4A_2}\!/_{4}\,Cos\left((2\omega_1+\omega_2)(t-\tau_5)+\varphi\right)+{}^{5A_1^4A_2}\!/_{4}\,Cos\left((2\omega_1-\omega_2)(t-\tau_5)-\varphi\right)\\
&+{}^{5A_1^4A_2}\!/_{16}\,Cos\left((4\omega_1+\omega_2)(t-\tau_5)+\varphi\right)+{}^{5A_1^4A_2}\!/_{16}\,Cos\left((4\omega_1-\omega_2)(t-\tau_5)-\varphi\right)\\
&+{}^{15A_1^3A_2^2}\!/_{4}\,Cos\left(\omega_1(t-\tau_5)\right)+{}^{15A_1^3A_2^2}\!/_{8}\,Cos\left((2\omega_2+\omega_1)(t-\tau_5)+2\varphi\right)\\
&+{}^{15A_1^3A_2^2}\!/_{8}\,Cos\left((2\omega_2-\omega_1)(t-\tau_5)+2\varphi\right)+{}^{5A_1^3A_2^2}\!/_{4}\,Cos\left(3\omega_1(t-\tau_5)\right)\\
&+{}^{5A_1^3A_2^2}\!/_{8}\,Cos\left((3\omega_1+2\omega_2)(t-\tau_5)+2\varphi\right)+{}^{5A_1^3A_2^2}\!/_{8}\,Cos\left((3\omega_1-2\omega_2)(t-\tau_5)-2\varphi\right)\\
&+{}^{15A_1^2A_2^3}\!/_{4}\,Cos\left(\omega_2(t-\tau_5)+\varphi\right)+{}^{5A_1^2A_2^3}\!/_{4}\,Cos\left(3\omega_2(t-\tau_5)+3\varphi\right)\\
&+{}^{15A_1^2A_2^3}\!/_{8}\,Cos\left((2\omega_1+\omega_2)(t-\tau_5)+\varphi\right)+{}^{15A_1^2A_2^3}\!/_{8}\,Cos\left((2\omega_1-\omega_2)(t-\tau_5)-\varphi\right)\\
&+{}^{5A_1^2A_2^3}\!/_{8}\,Cos\left((3\omega_2+2\omega_1)(t-\tau_5)+3\varphi\right)+{}^{5A_1^2A_2^3}\!/_{8}\,Cos\left((3\omega_2-2\omega_1)(t-\tau_5)+3\varphi\right)\\
&+{}^{15A_1A_2^4}\!/_{8}\,Cos\left(\omega_1(t-\tau_5)\right)+{}^{5A_1A_2^4}\!/_{4}\,Cos\left((2\omega_2+\omega_1)(t-\tau_5)+2\varphi\right)\\
&+{}^{5A_1A_2^4}\!/_{4}\,Cos\left((2\omega_2-\omega_1)(t-\tau_5)+2\varphi\right)+{}^{5A_1A_2^4}\!/_{16}\,Cos\left((4\omega_2+\omega_1)(t-\tau_5)+4\varphi\right)\\
&+{}^{5A_1A_2^4}\!/_{16}\,Cos\left((4\omega_2-\omega_1)(t-\tau_5)+4\varphi\right)+{}^{5A_2^5}\!/_{8}\,Cos\left(\omega_2(t-\tau_5)+\varphi\right)\\
&+{}^{5A_2^5}\!/_{16}\,Cos\left(3\omega_2(t-\tau_5)+3\varphi\right)+{}^{A_2^5}\!/_{16}\,Cos(\,5\omega_2(t-\tau_5)+5\varphi\,)]
\end{aligned}
\tag{3.5}
$$

Equation (3.5) presents amplitude and phase of frequency components that are produced by PA when it is excited with a two tone signal. Table 3-1 summarizes amplitudes and phases.

Table 3-1: Amplitude and Phase of Frequency Components Produced by PA

Frequency	Amplitude	Phase
ω_1	a_1A_1	$\omega_1(t-\tau_1)$
ω_2	a_1A_2	$\omega_2(t-\tau_1)+\varphi$
ω_1	$a_3\frac{3{A_1}^3}{4}+a_3\frac{3A_1A_2^2}{2}$	$\omega_1(t-\tau_3)$

Table 3-1 continues

Frequency	Amplitude	Phase
$3\omega_1$	$a_3\frac{A_1^3}{4}$	$3\omega_1(t-\tau_3)$
ω_1	a_1A_1	$\omega_1(t-\tau_1)$
ω_2	a_1A_2	$\omega_2(t-\tau_1)+\varphi$
ω_1	$a_3\frac{3A_1{}^3}{4}+a_3\frac{3A_1A_2^2}{2}$	$\omega_1(t-\tau_3)$
$3\omega_1$	$a_3\frac{A_1^3}{4}$	$3\omega_1(t-\tau_3)$
ω_2	$a_3\frac{3A_1^2A_2}{2}+a_3\frac{3A_2^3}{4}$	$\omega_2(t-\tau_3)+\varphi$
$2\omega_1+\omega_2$	$a_3\frac{3A_1^2A_2}{4}$	$(2\omega_1+\omega_2)(t-\tau_3)+\varphi$
$2\omega_1-\omega_2$	$a_3\frac{3A_1^2A_2}{4}$	$(2\omega_1-\omega_2)(t-\tau_3)-\varphi$
$2\omega_2+\omega_1$	$a_3\frac{3A_1A_2{}^2}{4}$	$(2\omega_2+\omega_1)(t-\tau_3)+2\varphi$
$2\omega_2-\omega_1$	$a_3\frac{3A_1A_2{}^2}{4}$	$(2\omega_2-\omega_1)(t-\tau_3)+2\varphi$
$3\omega_2$	$a_3\frac{A_2{}^3}{4}$	$3\omega_2(t-\tau_3)+3\varphi$
ω_1	$a_5\frac{5A_1^5}{8}+a_5\frac{15A_1^3A_2^2}{4}+a_5\frac{15A_1A_2^4}{8}$	$\omega_1(t-\tau_5)$
$3\omega_1$	$a_5\frac{5A_1^5}{16}+a_5\frac{5A_1^3A_2^2}{4}$	$3\omega_1(t-\tau_5)$
$5\omega_1$	$a_5\frac{A_1{}^5}{16}$	$5\omega_1(t-\tau_5)$
ω_2	$a_5\frac{15A_1^4A_2}{8}+a_5\frac{15A_1^2A_2^3}{4}+a_5\frac{5A_2^5}{8}$	$\omega_2(t-\tau_5)+\varphi$
$2\omega_1+\omega_2$	$a_5\frac{5A_1^4A_2}{4}+a_5\frac{15A_1^2A_2^3}{8}$	$(2\omega_1+\omega_2)(t-\tau_5)+\varphi$

Table 3-1 continues

$2\omega_1 - \omega_2$	$a_5\frac{5A_1^4A_2}{4} + a_5\frac{15A_1^2A_2^3}{8}$	$(2\omega_1 - \omega_2)(t-\tau_5) - \varphi$
$4\omega_1 + \omega_2$	$a_5\frac{5A_1^4A_2}{16}$	$(4\omega_1 + \omega_2)(t-\tau_5) + \varphi$
$4\omega_1 - \omega_2$	$a_5\frac{5A_1^4A_2}{16}$	$(4\omega_1 - \omega_2)(t-\tau_5) - \varphi$
$2\omega_2 + \omega_1$	$a_5\frac{15A_1^3{A_2}^2}{8} + a_5\frac{5A_1A_2^4}{4}$	$(2\omega_2 + \omega_1)(t-\tau_5) + 2\varphi$
$2\omega_2 - \omega_1$	$a_5\frac{15A_1^3{A_2}^2}{8} + a_5\frac{5A_1A_2^4}{4}$	$(2\omega_2 - \omega_1)(t-\tau_5) + 2\varphi$
$3\omega_1 + 2\omega_2$	$a_5\frac{5A_1^3{A_2}^2}{8}$	$(3\omega_1 + 2\omega_2)(t-\tau_5) + 2\varphi$
$3\omega_1 - 2\omega_2$	$a_5\frac{5A_1^3{A_2}^2}{8}$	$(3\omega_1 - 2\omega_2)(t-\tau_5) - 2\varphi$
$3\omega_2$	$a_5\frac{5A_1^2{A_2}^3}{4} + a_5\frac{5A_2^5}{16}$	$3\omega_2(t-\tau_5) + 3\varphi$
$3\omega_2 + 2\omega_1$	$a_5\frac{5A_1^2{A_2}^3}{8}$	$(3\omega_2 + 2\omega_1)(t-\tau_5) + 3\varphi$
$3\omega_2 - 2\omega_1$	$a_5\frac{5A_1^2{A_2}^3}{8}$	$(3\omega_2 - 2\omega_1)(t-\tau_5) + 3\varphi$
$4\omega_2 + \omega_1$	$a_5\frac{5A_1{A_2}^4}{16}$	$(4\omega_2 + \omega_1)(t-\tau_5) + 4\varphi$
$4\omega_2 - \omega_1$	$a_5\frac{5A_1{A_2}^4}{16}$	$(4\omega_2 - \omega_1)(t-\tau_5) + 4\varphi$
$5\omega_2$	$a_5\frac{{A_2}^5}{16}$	$5\omega_2(t-\tau_5) + 5\varphi$

It's seen in Table 3-1 that, three different terms which have unequal amplitude and unequal phase contribute to frequency component ω_1; this means that ω_1 frequency

component is the sum of three different terms. Figure 3-1 illustrates sum of unequal amplitude terms with unequal phase.

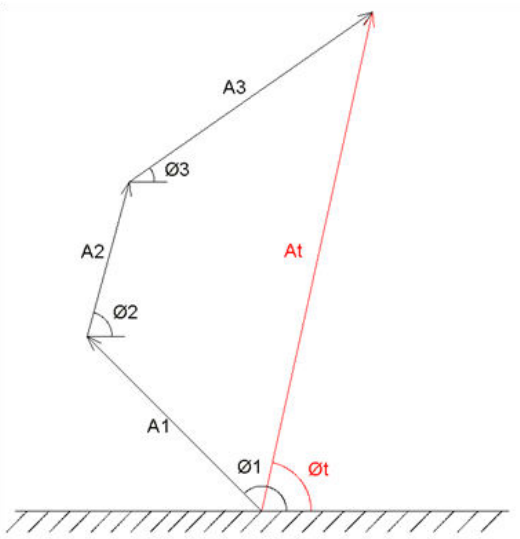

Figure 3-1 Sum of Unequal Amplitude Terms with Unequal Phase

$$A_1\angle\varphi_1 + A_2\angle\varphi_2 + A_3\angle\varphi_3 = A_t\angle\varphi_t \tag{3.6}$$

Table 3-2 summarizes frequency components at the output of PA and number of terms contributes to each frequency component.

Table 3-2: Frequency Components and Number of Terms Contribute to Frequency Components

Frequency	Number of Terms
ω_1	3
ω_2	3
$3\omega_1$	2
$2\omega_1 + \omega_2$	2
$2\omega_1 - \omega_2$	2
$2\omega_2 + \omega_1$	2
$2\omega_2 - \omega_1$	2
$3\omega_2$	2
$5\omega_1$	1
$4\omega_1 + \omega_2$	1

Table 3-2 continues

$4\omega_1 - \omega_2$	1
$3\omega_1 + 2\omega_2$	1
$3\omega_1 - 2\omega_2$	1
$3\omega_2 + 2\omega_1$	1
$3\omega_2 - 2\omega_1$	1
$4\omega_2 + \omega_1$	1
$4\omega_2 - \omega_1$	1
$5\omega_2$	1

Table 3-3 tabulates expressions for frequencies occurred at the output of PA when it is excited with a two-tone signal.

Table 3-3: Expression of Frequency Components Occurred at the Output of PA

Frequency	Expression
ω_1	$(a_1 A_1)e^{j\omega_1(t-\tau_1)} + (a_3\frac{3A_1^3}{4} + a_3\frac{3A_1A_2^2}{2})e^{j\omega_1(t-\tau_3)} + (a_5\frac{5A_1^5}{8} + a_5\frac{15A_1^3A_2^2}{4} + a_5\frac{15A_1A_2^4}{8})e^{j\omega_1(t-\tau_5)}$
ω_2	$(a_1 A_2)e^{j[\omega_2(t-\tau_1)+\varphi]} + (a_3\frac{3{A_1}^2A_2}{2} + a_3\frac{3A_2^3}{4})e^{j[\omega_2(t-\tau_3)+\varphi]} + (a_5\frac{15A_1^4A_2}{8} + a_5\frac{15A_1^2A_2^3}{4} + a_5\frac{5A_2^5}{8})e^{j[\omega_2(t-\tau_5)+\varphi]}$
$3\omega_1$	$(a_3\frac{{A_1}^3}{4})e^{j3\omega_1(t-\tau_3)} + (a_5\frac{5A_1^5}{16} + a_5\frac{5A_1^3A_2^2}{4})e^{j3\omega_1(t-\tau_5)}$
$2\omega_1 + \omega_2$	$(a_3\frac{3{A_1}^2A_2}{4})e^{j[(2\omega_1+\omega_2)(t-\tau_3)+\varphi]} + (a_5\frac{5A_1^4A_2}{4} + a_5\frac{15A_1^2A_2^3}{8})e^{j[(2\omega_1+\omega_2)(t-\tau_5)+\varphi]}$
$2\omega_1 - \omega_2$	$(a_3\frac{3{A_1}^2A_2}{4})e^{j[(2\omega_1-\omega_2)(t-\tau_3)-\varphi]} + (a_5\frac{5A_1^4A_2}{4} + a_5\frac{15A_1^2A_2^3}{8})e^{j[(2\omega_1-\omega_2)(t-\tau_5)-\varphi]}$

Table 3-3 continues

$2\omega_2+\omega_1$	$(a_3\frac{3A_1A_2^2}{4})e^{j[(2\omega_2+\omega_1)(t-\tau_3)+2\varphi]}+(a_5\frac{15A_1^3{A_2}^2}{8}+a_5\frac{5A_1A_2^4}{4})e^{j[(2\omega_2+\omega_1)(t-\tau_5)+2\varphi]}$
$2\omega_2-\omega_1$	$(a_3\frac{3A_1A_2^2}{4})e^{j[(2\omega_2-\omega_1)(t-\tau_3)+2\varphi]}+(a_5\frac{15A_1^3{A_2}^2}{8}+a_5\frac{5A_1A_2^4}{4})e^{j[(2\omega_2-\omega_1)(t-\tau_5)+2\varphi]}$
$3\omega_2$	$(a_3\frac{A_2^3}{4})e^{j[3\omega_2(t-\tau_3)+3\varphi]}+(a_5\frac{5A_1^2{A_2}^3}{4}+a_5\frac{5A_2^5}{16})e^{j[3\omega_2(t-\tau_5)+3\varphi]}$
$5\omega_1$	$(a_5\frac{A_1^5}{16})e^{j5\omega_1(t-\tau_5)}$
$4\omega_1+\omega_2$	$(a_5\frac{5A_1^4A_2}{16})e^{j[(4\omega_1+\omega_2)(t-\tau_5)+\varphi]}$
$4\omega_1-\omega_2$	$(a_5\frac{5A_1^4A_2}{16})e^{j[(4\omega_1-\omega_2)(t-\tau_5)-\varphi]}$
$3\omega_1+2\omega_2$	$(a_5\frac{5A_1^3{A_2}^2}{8})e^{j[(3\omega_1+2\omega_2)(t-\tau_5)+2\varphi]}$
$3\omega_1-2\omega_2$	$(a_5\frac{5A_1^3{A_2}^2}{8})e^{j[(3\omega_1-2\omega_2)(t-\tau_5)-2\varphi]}$
$3\omega_2+2\omega_1$	$(a_5\frac{5A_1^2{A_2}^3}{8})e^{j[(3\omega_2+2\omega_1)(t-\tau_5)+3\varphi]}$
$3\omega_2-2\omega_1$	$(a_5\frac{5A_1^2{A_2}^3}{8})e^{j[(3\omega_2-2\omega_1)(t-\tau_5)+3\varphi]}$
$4\omega_2+\omega_1$	$(a_5\frac{5A_1{A_2}^4}{16})e^{j[(4\omega_2+\omega_1)(t-\tau_5)+4\varphi]}$
$4\omega_2-\omega_1$	$(a_5\frac{5A_1{A_2}^4}{16})e^{j[(4\omega_2-\omega_1)(t-\tau_5)+4\varphi]}$
$5\omega_2$	$(a_5\frac{{A_2}^5}{16})e^{j[5\omega_2(t-\tau_5)+5\varphi]}$

Figure 3-2 illustrates frequency components occur around fundamentals and 3rd harmonics when a PA is excited with a two-tone signal.

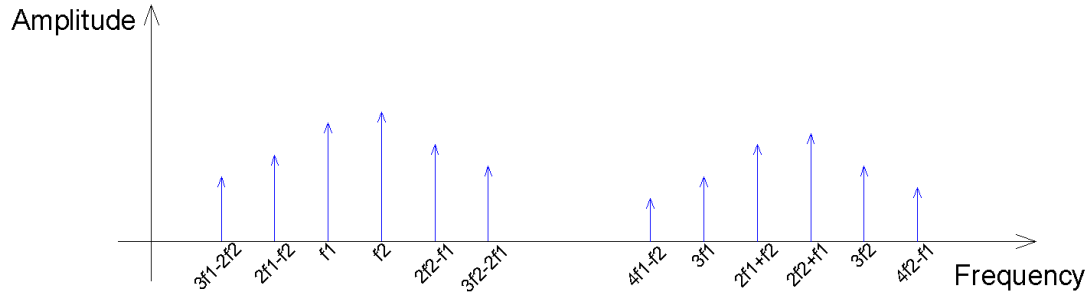

Figure 3-2 Frequency Components Occur at the Output of PA

In this section, model polynomial which is used for modeling purpose is introduced; amplitude and phase expressions of frequency components are derived.

In the next section, a new method which brings model polynomial parameters (coefficients and delay terms) is presented.

3.2 Parameter Extraction

Polynomial which relates input signal to output signal is given in the previous section. In this section, a method that brings model parameters to light is introduced.

Flowchart that is seen in Figure 3-3 shows steps of method which is used to find out model parameters.

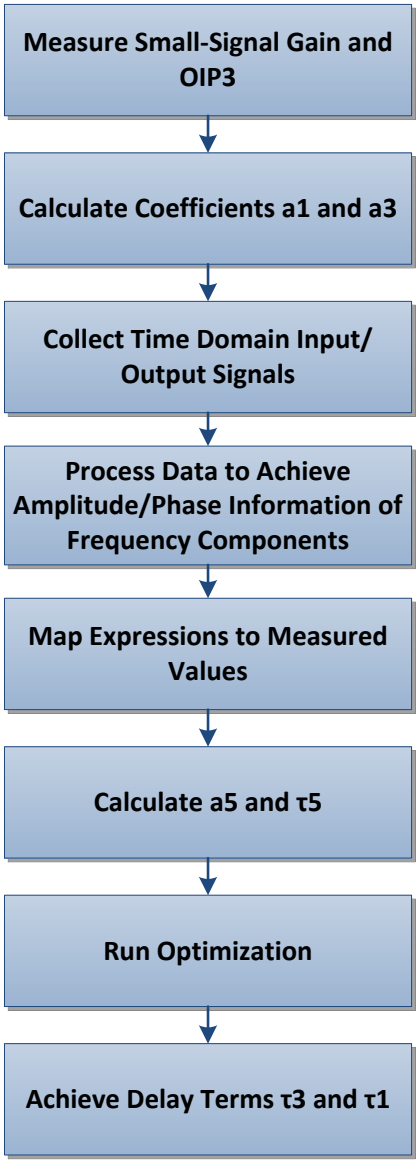

Figure 3-3 Steps of Model Construction

First of all, small signal gain and OIP_3 should be measured to calculate coefficients a_1 and a_3. Equations to calculate coefficients a_1 and a_3 are given below respectively;

$$a_1 = 10^{G/20} \tag{3.7}$$

$$a_3 = \frac{-2}{3R} 10^{\left(\frac{-OIP_3}{10} + \frac{3G}{20}\right)} \tag{3.8}$$

Next step is assembling a convenient measurement setup to collect time domain input and output signals. Time domain signals should be sampled with appropriate sampling rate. At step 4, FFT is used to move to frequency domain by this way it is possible to reach amplitude and phase of frequency components. In section 3.1 amplitude and phase expressions of frequency components are derived. Here expressions are mapped to measured data to calculate coefficient, a_5 and delay term, τ_5. By mapping expressions to measured data, coefficient a_5 and delay term τ_5 are achieved; however, it's not easy to find delay terms τ_1 and τ_3. Optimization is essential to reach these parameters. Primarily, an optimization procedure is run to identify delay term τ_3 and after reaching τ_3 another optimization procedure is run to find τ_1.

In continuing part of this section, mapping and optimization steps of parameter extraction procedure are explained in detail.

Amplitude of frequency component $3\omega_1 - 2\omega_2$ is $(a_5 \frac{5A_1^3 {A_2}^2}{8})$. It's seen that a_5, A_1 and A_2 determine the amplitude. Amplitude of frequency components $4\omega_1 + \omega_2$, $4\omega_1 - \omega_2$, $3\omega_1 + 2\omega_2$, $3\omega_2 + 2\omega_1$, $3\omega_2 - 2\omega_1$, $4\omega_2 + \omega_1$, $4\omega_2 - \omega_1$ and harmonics $5\omega_1, 5\omega_2$ are also product of a_5, A_1 and A_2. A_1 and A_2 are known parameters on this wise it is probable to achieve coefficient a_5 using amplitude of any frequency components listed above. On the other hand, amplitude of low frequency intermodulations is higher than amplitude of high frequency intermodulations. Therefore, it's convenient to use frequency components $3\omega_1 - 2\omega_2$, $3\omega_2 - 2\omega_1$ instead of $5\omega_1$, $4\omega_1 + \omega_2$, $4\omega_1 - \omega_2$ etc. in calculations because measurement error is smaller for these frequencies.

Phase of $3\omega_1 - 2\omega_2$ is $(3\omega_1 - 2\omega_2)(t - \tau_5) - 2\varphi$. At a reference time $t = 0$; $\omega_1, \omega_2, \tau_5$ and φ contribute to phase. ω_1, ω_2 are known, φ can be obtained with measurement. As a result, it is possible to achieve τ_5 using phase of $3\omega_1 - 2\omega_2$. This procedure is also applicable for frequency components $5\omega_1$, $4\omega_1 + \omega_2$, $4\omega_1 - \omega_2$, $3\omega_1 + 2\omega_2$, $3\omega_2 + 2\omega_1$, $3\omega_2 - 2\omega_1$, $4\omega_2 + \omega_1$, $4\omega_2 - \omega_1$ and $5\omega_2$. In the previous paragraph, it's stated that using frequency components that have higher

amplitudes is convenient to extract model parameters because measurement error is smaller on these frequencies. Add to this, it is adequate to use phases of frequencies which have more accurate amplitude information because phase of a frequency component is accurate if amplitude of that component is accurate. Therefore, using phases of $3\omega_1 - 2\omega_2$ and $3\omega_2 - 2\omega_1$ is more suitable to arrive missing parameter τ_5.

Frequency component $2\omega_1 - \omega_2$ is represented with a summation $(a_3 \frac{3{A_1}^2 A_2}{4}) e^{j[(2\omega_1-\omega_2)(t-\tau_3)-\varphi]} + (a_5 \frac{5A_1^4 A_2}{4} + a_5 \frac{15A_1^2 A_2^3}{8}) e^{j[(2\omega_1-\omega_2)(t-\tau_5)-\varphi]}$. First part of summation is $(a_3 \frac{3{A_1}^2 A_2}{4}) e^{j[(2\omega_1-\omega_2)(t-\tau_3)-\varphi]}$; amplitude is known but phase is unknown because of τ_3. Second part of summation is $(a_5 \frac{5A_1^4 A_2}{4} + a_5 \frac{15A_1^2 A_2^3}{8}) e^{j[(2\omega_1-\omega_2)(t-\tau_5)-\varphi]}$; both amplitude and phase is known. It is possible to find phase of the first part by running optimization if amplitude and phase of frequency component $2\omega_1 - \omega_2$ are measured. τ_3 is obtained when phase is achieved.

$$A\angle B = Ae^{jB} \tag{3.9}$$

$$Ae^{jB} = ACosB + jASinB \tag{3.10}$$

$$\begin{aligned} Known1\angle Unknown + Known2\angle Known3 \\ = Known4\angle Known5 \end{aligned} \tag{3.11}$$

Equation (3.11) summarizes problem. In brief, aim of optimization is achieving unknown phase thereby achieving τ_3.

In Figure 3-4, exact $2\omega_1 - \omega_2$ and approximate $2\omega_1 - \omega_2$ are shown as points on complex numbers domain. The method varies phase of approximate $2\omega_1 - \omega_2$ and monitor distance; phase which makes distance smaller is closer to the exact phase.

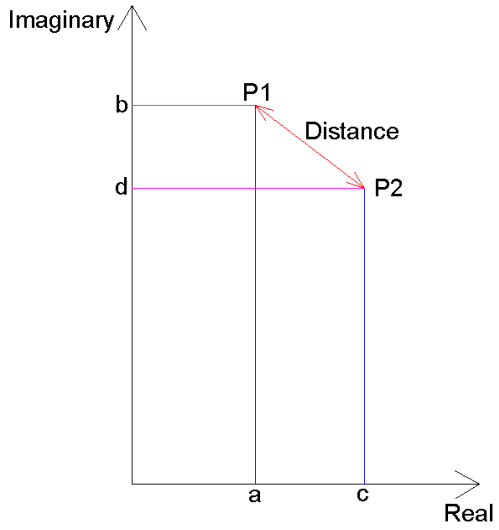

Figure 3-4 Illustration of Optimization

$$Distance = \sqrt{(c-a)^2 + (b-d)^2} \tag{3.12}$$

Above steps describe the way to find parameters a_5, τ_5 and τ_3. There is one unknown remained, τ_1. ω_1 frequency component is represented with expression; $(a_1 A_1) e^{j\omega_1(t-\tau_1)} + \left(a_3 \frac{3{A_1}^3}{4} + a_3 \frac{3A_1A_2^2}{2}\right) e^{j\omega_1(t-\tau_3)} + \left(a_5 \frac{5A_1^5}{8} + a_5 \frac{15A_1^3A_2^2}{4} + a_5 \frac{15A_1A_2^4}{8}\right) e^{j\omega_1(t-\tau_5)}$. At a reference time $t = 0$, every parameter except τ_1 is known. If amplitude and phase of ω_1 are measured then optimization procedure brings a close value to τ_1.

In this section, methodology used to identify model parameters is described step by step.

3.3 Measurement Setup

Measurement setup which is used to collect appropriate data will be introduced in this section. Figure 3-5 shows configuration of measurement setup.

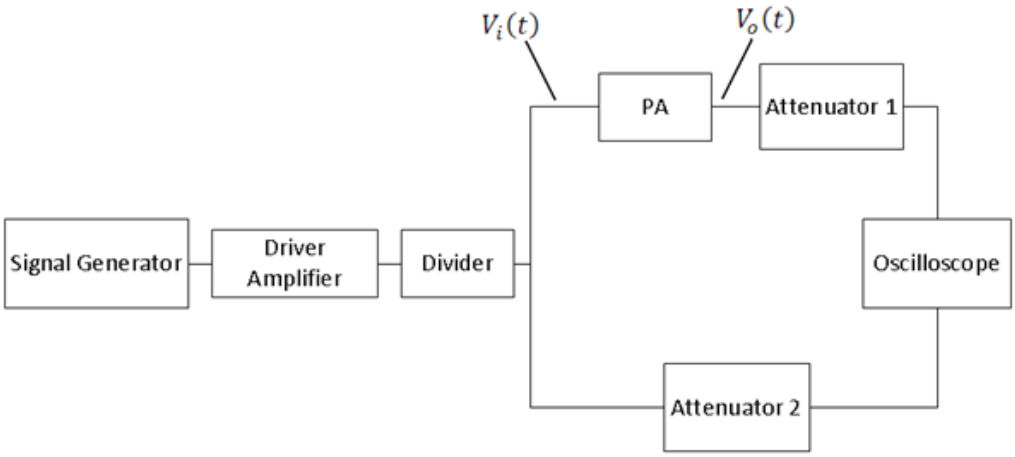

Figure 3-5 Configuration of Measurement Setup

Primarily, a signal generator which has ability to produce multi-tone signal produces two-tone signal then a driver amplifier amplifies the produced signal. Driver amplifier should satisfy two conditions; it should work in linear region and it shouldn't create memory. Only nonlinearity and memory source should be PA. Subsequently, an in-phase power divider is used to build two different paths to sample both at the same time: input and output time domain signals. Attenuators which are used in both paths decrease power level not to harm the oscilloscope. Setup ends up with an oscilloscope which samples both data coming from different paths.

Setup assembled in laboratory of Aselsan Inc. is seen in Figure 3-6.

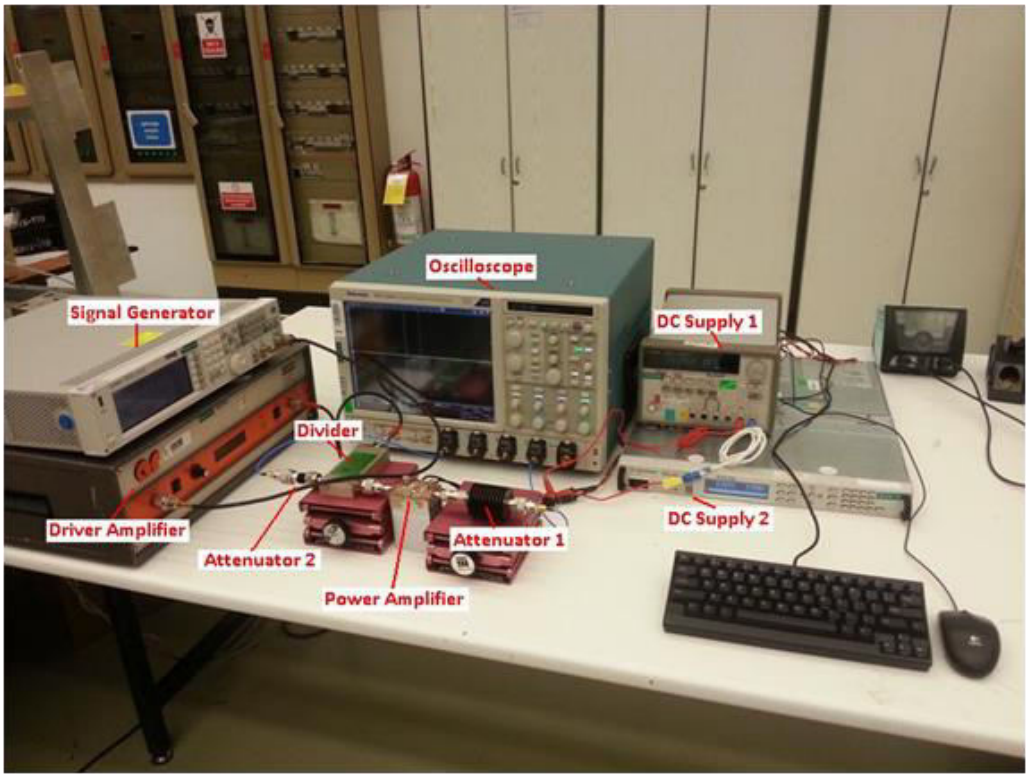

Figure 3-6 Measurement Setup

PA which is used for modeling purpose is 1-2GHz, 10W saturated output power class AB type amplifier. Oscilloscope should have high sampling rate capability to sample signals between 1-2GHz. It samples and records time domain input and output signals then Fourier Transform in MATLAB is used to move to frequency domain. Transform brings ability to achieve amplitude/phase of fundamentals, harmonics and intermodulation products.

Nyquist Sampling Theorem states that sampling frequency should be at least two times of the highest interested frequency.

$$F_s \geq 2F_{highest} \tag{3.13}$$

It's planned to perform measurements for modeling purpose at $1.5GHz$ center frequency. For $16MHz$ frequency separation, highest interested frequency is $4.54GHz$. Thus, sampling frequency should be greater than $9.08GHz$.

Resolution of frequency spectrum is described by sampling frequency and record length. The formula for resolution is;

$$Res = \frac{F_s}{N} \tag{3.14}$$

Increasing record length or decreasing sampling frequency is necessary to improve resolution. However, sampling frequency has to be at least two times of highest interested frequency; there is a trade-off here. An optimal sampling frequency and record length should be decided.

Figure 3-7 shows spectrum of signal after FFT. $F_s/_2$ is the upper frequency limit.

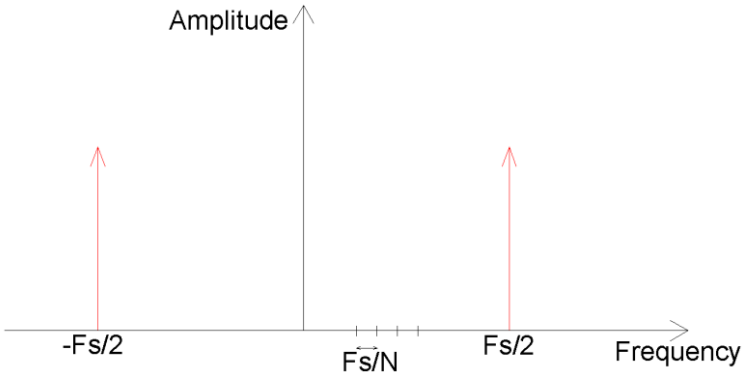

Figure 3-7 Frequency Spectrum of Signal after FFT

CHAPTER 4

RESULTS

4.1 Identified Model Parameters

Setup which is assembled to perform measurements is introduced in the previous section. In this chapter, data that is collected from various measurements and results that are achieved with model construction method are presented. Achieved parameters and calculated delay terms are declared.

The first step of model construction procedure is to find coefficients a_1 and a_3. Previously, equations (3.7) and (3.8) are given to calculate these coefficients. Table 4-1 presents results of OIP_3 and small signal gain measurements performed for $2MHz$ and $16MHz$ frequency separation.

Table 4-1: Results of OIP_3 and Gain Measurement

Frequency Separation (MHz)	Input Power (dBm)	Output Power (dBm)	IMD Term (dBm)	IMD (dBc)	OIP_3 (dBm)	Gain (dB)
2	21.2	31.3	-13.3	44.6	53.6	13.1
16		31.4	-12.4	43.8	53.3	13.2

Table 4-2: Calculated coefficients

Frequency Separation (MHz)	a_1	a_3
2	4.519	-0.0053
16	4.571	-0.0059

Table 4-2 presents calculated values of a_1, a_3 for $2MHz$ and $16MHz$ frequency separation conditions.

Remaining steps of the procedure follow measurements which are performed to collect appropriate data.

Three different measurements are performed to investigate three different cases. First of all bandwidth of two tone excitation signal is adjusted to $2MHz$ and parameters of model are extracted for this condition. Second measurement is performed again with $2MHz$ signal bandwidth to verify consistency of measurements and model construction method. Third measurement is performed with $16MHz$ frequency separation to see the variation of coefficients and delay terms with respect to signal bandwidth.

Settings of Measurement-1A;

$f = 1.5GHz$
$F_s = 12.5x10^9\ Hz$
$N = 25000$
$F_{sep} = 2MHz$
$Res = 0.5MHz$

f is center frequency, F_s is sampling frequency of the oscilloscope, N is record length, F_{sep} is frequency separation and Res is the resolution of the spectrum.

In Figure 4-1, measured time domain input and output signals are seen.

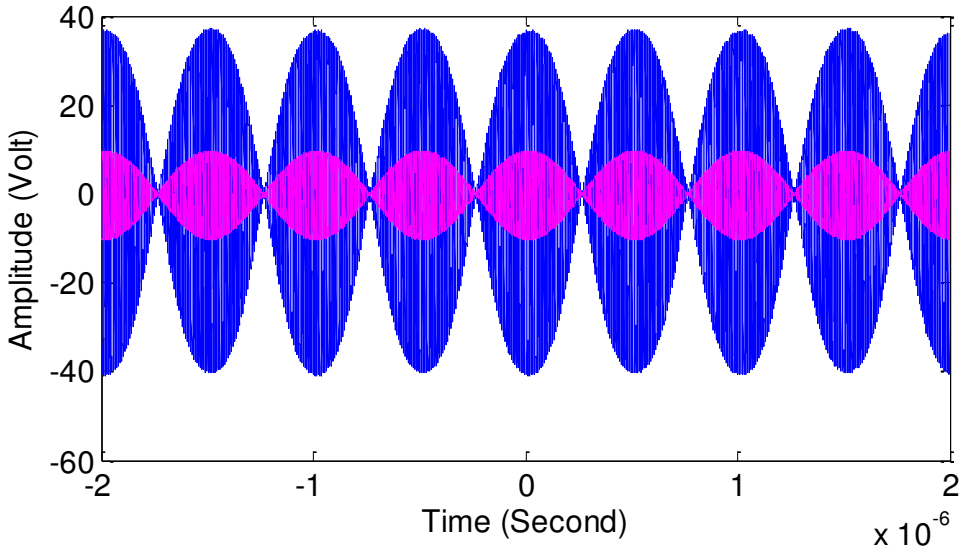

Figure 4-1 Measured Time Domain Input Signal (magenta) and Measured Time Domain Output Signal (blue) for Measurement-1A

While performing measurements, input and output time domain signals are captured simultaneously; waveforms are recorded into a file which is suitable to process in MATLAB.

FFT transform is a well-known method to convert time domain signal to frequency domain signal. Transform is useful to achieve amplitude and phase of frequency components. However, fft function in MATLAB doesn't bring the exact phase of frequency component; the phase which transform brings involves extra terms within.

Erdal Mehmetcik (a colleague in Aselsan Inc.) has studied this issue in his M. Sc. Thesis and has written two different MATLAB scripts instead of fft function. One of the scripts is simple to execute but other costs more computational load. Both scripts bring real amplitude/phase of frequency components. The one which requires less computational load is used to identify amplitude/phase of fundamentals, harmonics and intermodulations.

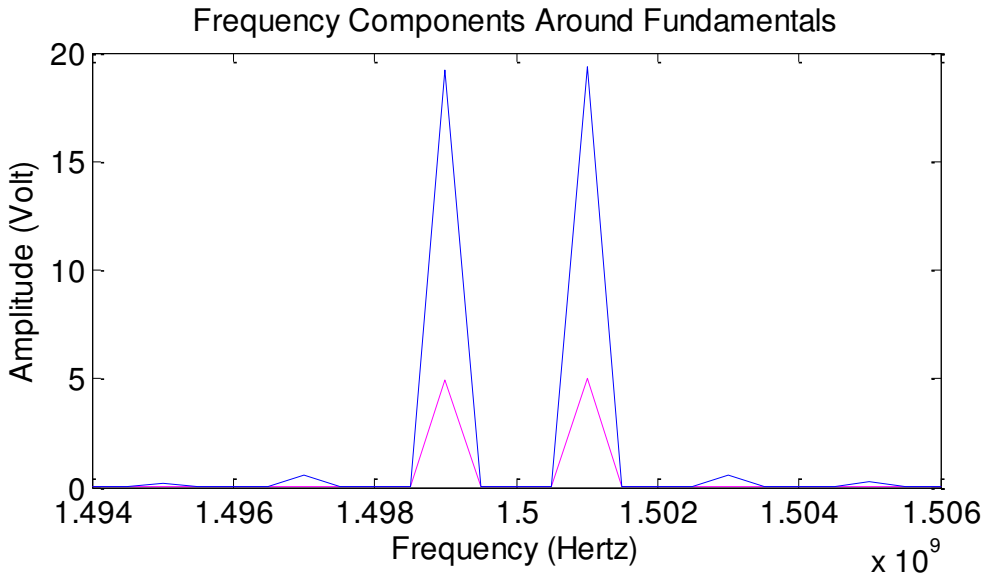

Figure 4-2 Frequency Components around Fundamentals for Measurement-1A (magenta/Input Signal, blue/Output Signal)

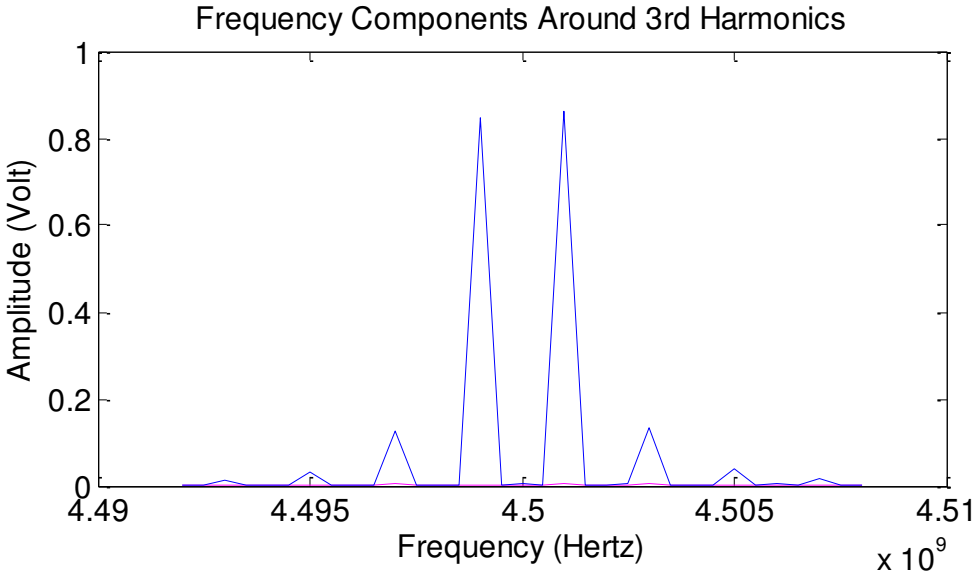

Figure 4-3 Frequency Components around 3rd Harmonics for Measurement-1A (magenta/Input Signal, blue/Output Signal)

In Figure 4-2, fundamentals and intermodulation products occur around fundamentals such $3\omega_1 - 2\omega_2$, $2\omega_1 - \omega_2$, $2\omega_2 - \omega_1$ and $3\omega_2 - 2\omega_1$ are seen.

In Figure 4-3, intermodulation products occur around 3rd harmonics such $4\omega_1 - \omega_2$, $2\omega_1 + \omega_2$, $2\omega_2 + \omega_1$ and $4\omega_2 - \omega_1$ are seen. Harmonics and intermodulation

products aren't seen at the input signal, they occur at the output signal because of nonlinearity.

Table 4-3: Amplitude/Phase of Frequency Components of Measured Input Signal and Measured Output Signal for Measurement-1A

2MHz										
Input Signal				Output Signal						
Fundamentals				Fundamentals and Intermodulations						
	Frequency (MHz)	Amplitude (V)	Phase (°)		Frequency (MHz)	Amplitude (V)	Phase (°)			
f1	1499	4,9500	136,9	f1	1499	19,2100	-52,6			
f2	1501	5,0000	125,6	f2	1501	19,3800	-64,7			
				2f1-f2	1497	0,5430	139,8			
				2f2-f1	1503	0,5450	107,4	a5		
				3f1-2f2	1495	0,2170	153,4	3f1-2f2	0,00011	Average
				3f2-2f1	1505	0,2280	90,2	3f2-2f1	0,00012	0,00012

Table 4-3 tabulates amplitude/phase of frequency components of measured input signal and measured output signal.

In input signal, amplitude of fundamentals f_1 and f_2 are close; also phase of fundamentals are close.

In output signal amplitude/phase of fundamentals f_1 and f_2 are close. Amplitudes of frequency components $2f_1 - f_2$, $2f_2 - f_1$ are close however, phases of these terms are different. Besides, amplitudes of $3f_1 - 2f_2$, $3f_2 - 2f_1$ are close phases of these terms are different. Unequal phases are the result of memory effect.

Two different equations exist to calculate coefficient a_5; Table 4-3 shows coefficients a_5 that are calculated with these equations. In the forthcoming calculations, arithmetic mean of calculated a_5 values is used.

Table 4-4: Amplitude/Phase of Frequency Components of Measured Output Signal for Measurement-1A

2MHz						
Frequency	Amplitude (V)	Phase Expression (radian)	Phase Expression (°)	Amplitude (V)	Phase (radian)	Phase (°)
ω1	22,37	(-2π*f1)*(τ1)	-f1*(τ1)*360	19,210	-0,92	-52,60
	-1,47	(-2π*f1)*(τ3)	-f1*(τ3)*360			
	2,28	(-2π*f1)*(τ5)	-f1*(τ5)*360			
ω2	22,60	(-2π*f2)*(τ1)+φ	[((-2π*f2)*(τ1)+φ)/π]*180	19,380	-1,13	-64,70
	-1,47	(-2π*f2)*(τ3)+φ	[((-2π*f2)*(τ3)+φ)/π]*180			
	2,29	(-2π*f2)*(τ5)+φ	[((-2π*f2)*(τ5)+φ)/π]*180			
2ω1-ω2	-0,49	(-2π*(2f1-f2))*(τ3)-φ	[((-2π*(2f1-f2))*(τ3)-φ)/π]*180	0,543	2,44	139,80
	1,14	(-2π*(2f1-f2))*(τ5)-φ	[((-2π*(2f1-f2))*(τ5)-φ)/π]*180			
2ω2-ω1	-0,49	(-2π*(2f2-f1))*(τ3)+2φ	[((-2π*(2f2-f1))*(τ3)+2φ)/π]*180	0,545	1,87	107,40
	1,15	(-2π*(2f2-f1))*(τ5)+2φ	[((-2π*(2f2-f1))*(τ5)+2φ)/π]*180			
3ω1-2ω2	0,23	(-2π*(3f1-2f2))*(τ5)-2φ	[((-2π*(3f1-2f2))*(τ5)-2φ)/π]*180	0,217	2,68	153,40
3ω2-2ω1	0,23	(-2π*(3f2-2f1))*(τ5)+3φ	[((-2π*(3f2-2f1))*(τ5)+3φ)/π]*180	0,228	1,57	90,20

Table 4-4 presents amplitude/phase of frequency components of measured output signal. 2nd column shows amplitude of terms that contribute to the frequency components. Phase expressions in radian are seen in 3rd column and phase expressions in degree are seen in 4th column.

Calculations are done, optimization procedure is run; coefficients and delay terms are achieved.

Table 4-5 presents model coefficients and delay terms which are achieved.

Table 4-5: Model Polynomial Coefficients and Delay Terms Achieved for Measurement-1A

2MHz		
Coefficients	a_1	4.519
	a_3	-0.0053
	a_5	0.00012
Delay Terms	τ_1	93ps
	τ_3	179ps
	τ_5	216ps

According to the results shown in Table 4-5; model polynomial can be written as;

$$V_o(t) = 4.519V_i(t - 93x10^{-12}) - 0.0053V_i^3(t - 179x10^{-12}) + 0.00012V_i^5(t - 216x10^{-12}) \quad (4.1)$$

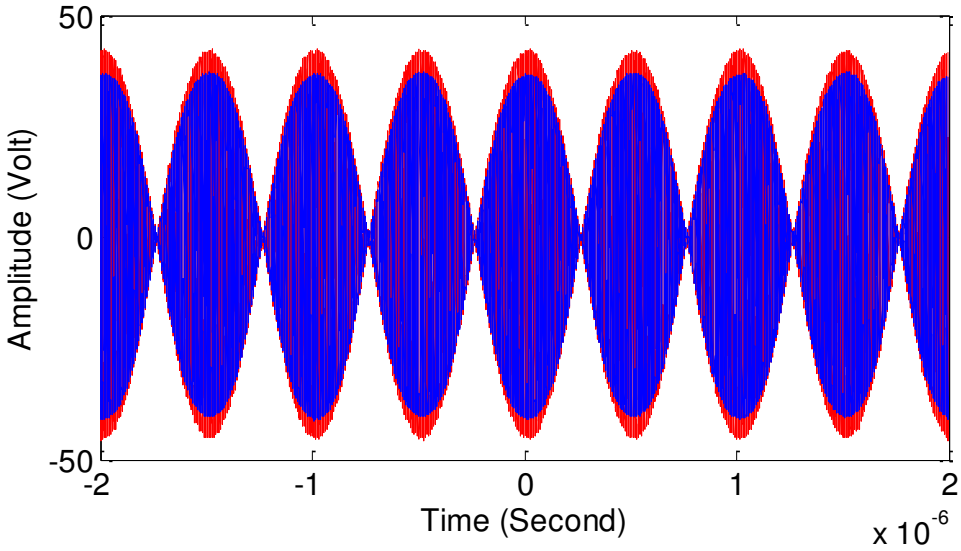

Figure 4-4 Measured Time Domain Output Signal (blue) and Simulated Time Domain Output Signal (red) for Measurement-1A

Figure 4-4 shows measured time domain output signal and simulated time domain output signal. It is seen in Figure 4-4 that simulated and measured time domain output signals are close to each other. A difference is seen at the peak of the envelope of the signals but in a general manner simulated time domain output signal follows measured time domain output signal. This is promising for the usefulness of the model.

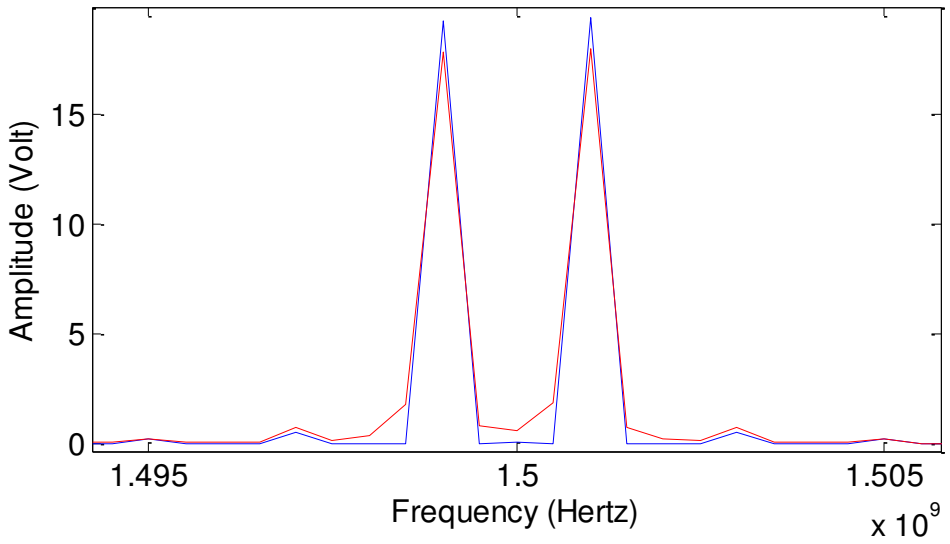

Figure 4-5 Frequency Spectrum of Measured Output Signal (blue) and Simulated Output Signal (red) Around Fundamentals for Measurement-1A

Figure 4-5 presents frequency spectrum of measured output signal and simulated output signal around fundamentals.

It is seen in Figure 4-5 that amplitude of measured frequency domain output signal and amplitude of simulated frequency domain output signal are close. There is no frequency shift seen in the spectrum. Amplitudes of fundamentals are almost same.

Table 4-6: Comparison of Amplitude/Phase of Measured Output Signal and Simulated Output Signal for Measurement-1A

Measured Output Signal				Simulated Output Signal		
Frequency	Amplitude (V)	Phase (radian)	Phase (°)	Amplitude (V)	Phase (radian)	Phase (°)
ω1	19,21	-0,92	-52,60	17,80	2,33	133,40
ω2	19,38	-1,13	-64,70	17,94	2,13	122,20
2ω1-ω2	0,543	2,44	139,80	0,721	0,82	47,10
2ω2-ω1	0,545	1,87	107,40	0,703	0,19	10,80
3ω1-2ω2	0,217	2,68	153,40	0,205	1,26	72,30
3ω2-2ω1	0,228	1,57	90,20	0,186	0,22	12,55

Table 4-6 compares amplitude/phase of measured output signal and simulated output signal.

Amplitude of frequency components of the simulated output signal and amplitude of frequency components of the measured output signal is close. Phases are not exactly same but phase difference between frequency pairs such $2\omega_1 - \omega_2$ and $2\omega_2 - \omega_1$ are close for both signals.

To test repeatability and consistency, another measurement is performed with same settings at a different time. Results of intermediate steps can be found in the Appendix.

Table 4-7: Model Polynomial Coefficients and Delay Terms Achieved for Measurement-1B

2MHz		
Coefficients	a_1	4.519
	a_3	-0.0053
	a_5	0.00012
Delay Terms	τ_1	88ps
	τ_3	169ps
	τ_5	205ps

According to the Table 4-7, model polynomial can be written as;

$$V_o(t) = 4.519V_i(t - 88x10^{-12}) - 0.0053V_i^3(t - 169x10^{-12}) + 0.00012V_i^5(t - 205x10^{-12}) \quad (4.2)$$

Results of Measurement-1B are parallel with the results of Measurement-1A. Model polynomials denoted with equations (4.1) and (4.2) are almost same. These results are evidence of repeatability and consistency.

To investigate the relation between bandwidth of excitation signal and delay terms, another measurement is performed. This time frequency separation between tones is $16MHz$.

Settings of Measurement-2;

$f = 1.5GHz$
$F_s = 12.5x10^9\,Hz$
$N = 25000$
$F_{sep} = 16MHz$
$Res = 0.5MHz$

f is center frequency, F_s is sampling frequency of the oscilloscope, N is record length, F_{sep} is frequency separation between tones and Res is resolution of the

spectrum. Tables showing data which are achieved at the intermediate steps can be seen in the Appendix.

Steps that are summarized in Figure 3-3 are applied and model polynomial parameters which are shown in Table 4-8 are achieved.

Coefficients $a_{1,}a_3$ and a_5 don't change prominently; however, delay terms τ_1, τ_2 and τ_3 increase noticeably when bandwidth of signal (separation between tones) increases. This means that memory is more effective when PA is excited with a wider band signal. This type of memory is short term memory and especially called as 'electrical memory'.

Table 4-8: Model Polynomial Coefficients and Delay Terms Achieved for Measurement-2

16MHz		
Coefficients	a_1	4.571
	a_3	-0.0059
	a_5	0.00011
Delay Terms	τ_1	111ps
	τ_3	192ps
	τ_5	231ps

Coefficients and delay terms that are calculated for 16MHz excitation signal bandwidth are different than coefficients and delay terms that are calculated for 2MHz excitation signal bandwidth. Expectation is realized; delay terms are increased depending on the increase of signal bandwidth.

According to the Table 4-8, model polynomial can be written as;

$$V_o(t) = 4.571V_i(t - 111x10^{-12}) - 0.0059V_i^3(t - 192x10^{-12}) + 0.00011V_i^5(t - 231x10^{-12}) \quad (4.3)$$

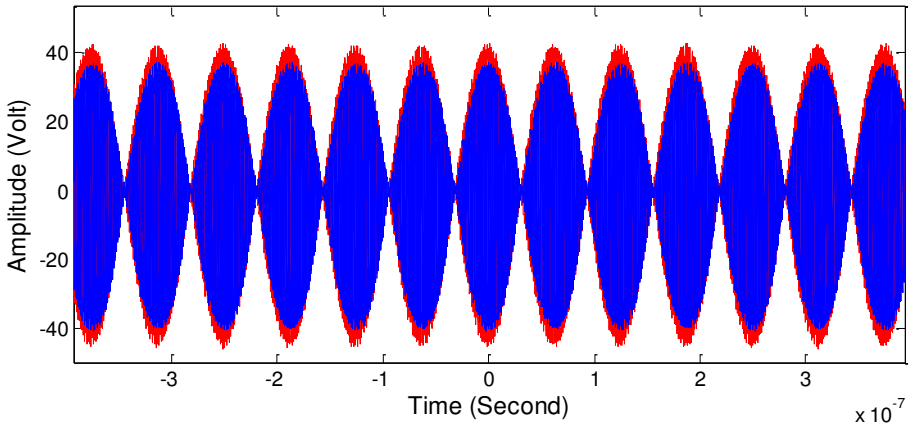

Figure 4-6 Measured Time Domain Output Signal (blue) and Simulated Time Domain Output Signal (red) for Measurement-2

Envelope of simulated time domain output signal and measured time domain output signal are seen in Figure 4-6. A difference between amplitudes is seen at the peaks of the sinusoids however, there is no big phase shift seen in the figure. Simulated signal follows the measured signal quite well.

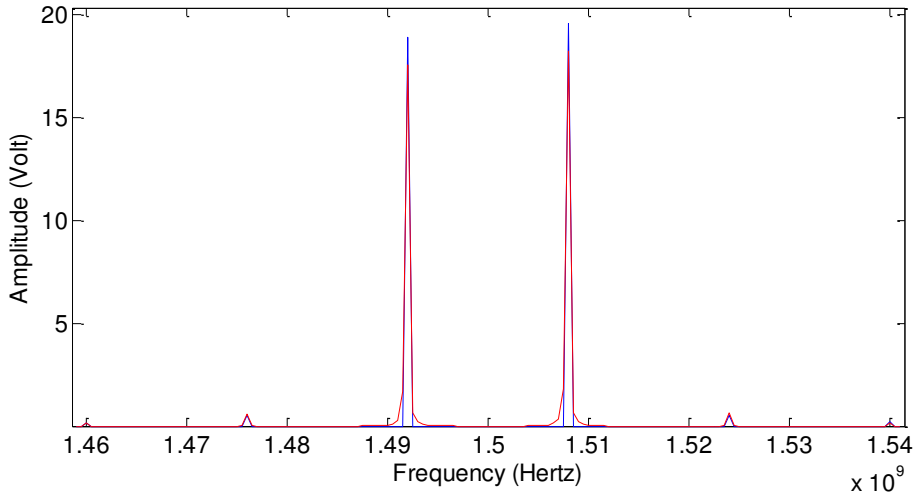

Figure 4-7 Frequency Spectrum of Measured Output Signal (blue) and Simulated Output Signal (red) Around Fundamentals for Measurement-2

Frequency spectrum of measured and simulated output signals around fundamentals is seen in Figure 4-7. Difference between fundamental frequency components of two different signals is small. There is no frequency shift seen in the figure. Simulated signal follows measured signal quite well.

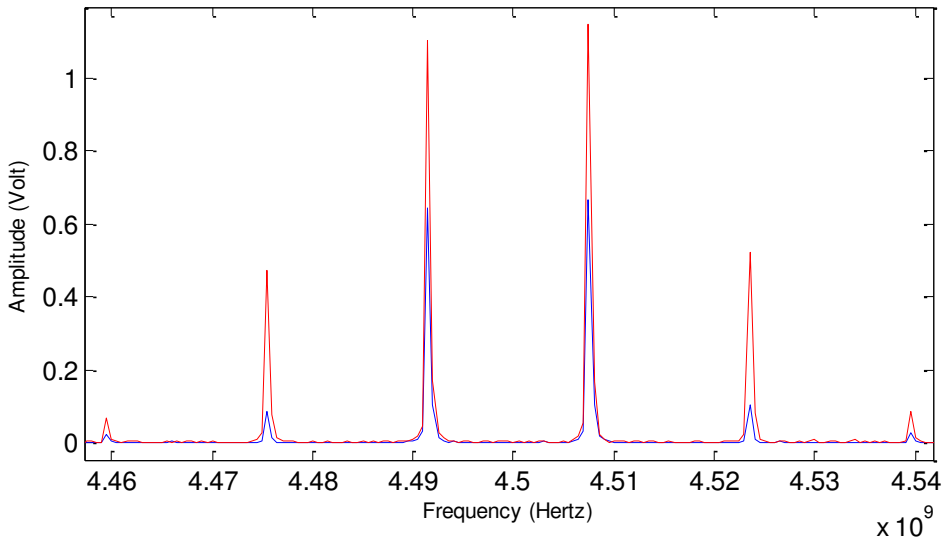

Figure 4-8 Frequency Spectrum of Measured Output Signal (blue) and Simulated Output Signal (red) Around 3rd Harmonics for Measurement-2

Figure 4-8 shows frequency spectrum of measured output signal and simulated output signal around 3rd harmonics for Measurement-2. Amplitude of intermodulation products of simulated and measured output signals is close but not exactly same. The method which is used to extract parameters utilizes time domain input and output signals whose frequency is 1.5GHz however; method is capable of modeling the response of the PA around harmonic frequencies.

Table 4-9: Comparison of Amplitude/Phase of Measured Output Signal and Simulated Output Signal for Measurement-2

Measured Output Signal				Simulated Output Signal		
Frequency	Amplitude (V)	Phase (radian)	Phase (°)	Amplitude (V)	Phase (radian)	Phase (°)
ω1	18,910	-1,03	-59,30	17,560	2,18	125,07
ω2	19,580	-1,01	-58,10	18,190	2,30	132,04
2ω1-ω2	0,564	1,99	114,30	0,618	0,12	6,94
2ω2-ω1	0,520	2,32	133,00	0,641	0,43	24,78
3ω1-2ω2	0,188	2,18	125,20	0,169	0,44	25,39
3ω2-2ω1	0,229	2,06	118,10	0,173	0,85	48,80

Table 4-9 compares amplitude/phase of measured output signal and simulated output signal for Measurement-2. Amplitudes of frequency components of two different signals are close. Phase of frequency components are not same however; phase difference between frequency component pairs are similar.

One of the most significant things about this study is calculating the model parameters analytically. This is the contribution of the study. These parameters haven't been declared before.

In this section, parameters of the model polynomial are calculated by using an analytic method. Measurements that are performed at different times with same settings produce almost same data. Proposed method produces same coefficients and delay terms with the data which is collected at different time. These are evidences of consistency and repeatability.

Relation between bandwidth of excitation signal and delay terms is enlightened in this section. Increasing bandwidth of excitation signal causes increase of delay terms. In short, results that are presented verify the expectations.

4.2 Validity of the Model

In the previous sections, coefficients and delay terms are identified with parameter extraction procedure, memory model is constructed and results that are achieved with proposed model are presented. In this section, model will be tested with a method to discover the success of the modeling.

NMSE in long form Normalized Mean Square Error is a general criterion that is used to test success of modeling approaches. In some applications, it is used to tune model parameters. Equation (2.3) given in section 2.1.2 describes how to calculate NMSE. If a model is successful then evaluated NMSE is closer to minus infinity. Table below shows NMSE values which are calculated for different measurements.

Table 4-10: Calculated NMSE Values for Frequency Domain

	Model I	Model II	Model III
NMSE	-27,9dB	-27,7dB	-28,3dB

NMSE values that are seen in Table 4-10 are calculated by using frequency domain amplitude of measured output signal and frequency domain amplitude of simulated output signal.

Table 4-11: Calculated NMSE Values for Time Domain

	Model I	Model II	Model III
NMSE	-15,2dB	-14,9dB	-15,7dB

NMSE values that are seen in Table 4-11 are calculated by using measured time domain output signal and simulated time domain output signal.

Model I is built on the data which is gathered from Measurement-1A, Model II is built on the data which is gathered from Measurement-1B and Model III is built on the data which is gathered from Measurement-2. NMSE values that are seen in Table 4-10 and Table 4-11 show that the approach which is applied to build a model is acceptable.

NMSEs that are calculated with frequency domain signals are better than the NMSEs calculated with time domain signals. Success of modeling is better in frequency domain. NMSEs are good, but not perfect. Capability of proposed model is limited. Using higher order terms or adding even orders terms can improve the success of modeling.

Further, increasing the data length or increasing the sampling rate while performing measurements can improve measurement accuracy and cause a better modeling.

One other option to achieve better NMSEs is to change measurement setup. A better measurement setup can be configured to lower measurement errors.

4.3 Relation Between Bias Circuit Components and Delay Terms

It is known that bias circuit components affect delay terms. Memory of PA changes depending on the magnetic flux storing or charge storing components (capacitors, inductors). Bias circuit influences electrical memory –short term memory- especially. In this section, relation between bias circuit components and delay terms is investigated.

Controlled experiment method is applied to observe effect of bias circuit components on memory. Bias circuit component is changed providing that the other circuit components stay same. Under this condition variations of delay terms are observed.

Schematic of the PA is given in Figure 4-9. Circuit components whose effects are investigated are encircled.

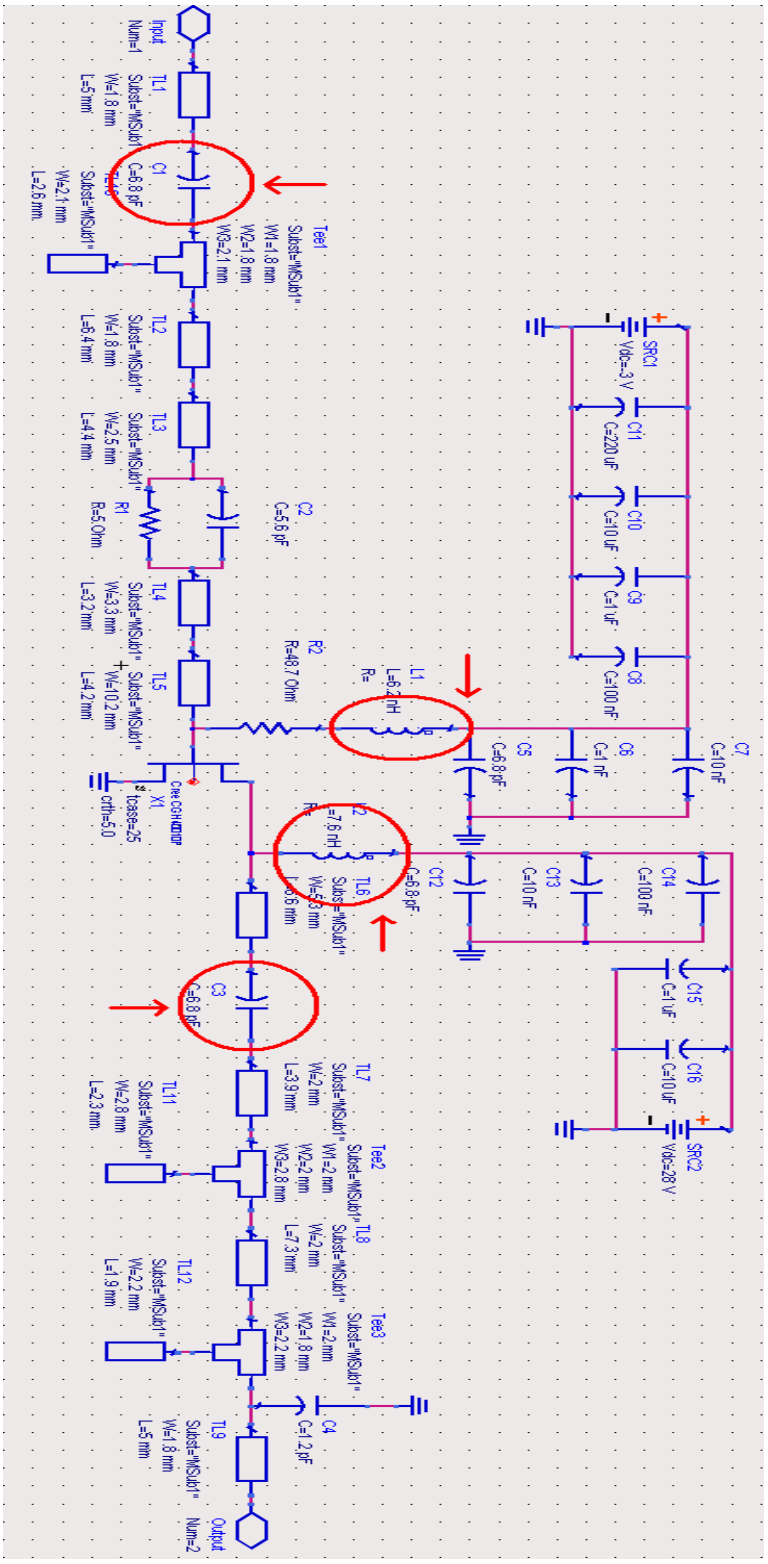

Figure 4-9 Schematic of the PA

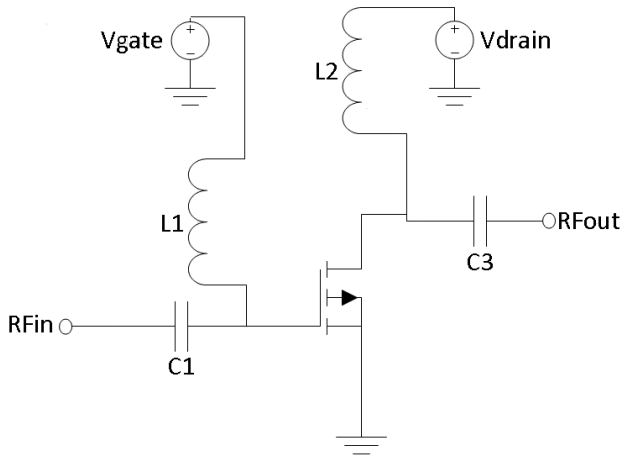

Figure 4-10 Simplified Circuit of PA

The simplified circuit of PA which is used for modeling purpose is given in Figure 4-10. L1 and C1 are the components of input bias circuit; L2 and C3 are the components of output bias circuit.

Table 4-12: Initial Values of Coefficients and Delay Terms

16MHz		
Coefficients	a_1	4.571
	a_3	-0.0059
	a_5	0.0001
Delay Terms	τ_1	91ps
	τ_3	195ps
	τ_5	242ps

Table 4-12 presents initial values of coefficients and delay terms. For the first case, capacitor of input bias circuit C1 is changed from 6.8pF to 30pF. Delay terms and variations of delay terms with respect to the initial values can be seen in Table 4-13.

Table 4-13: Coefficients and Delay Terms of Case-1

C1			
Coefficients	a_1	4.571	
	a_3	-0.0059	
	a_5	0.0001	
Delay Terms	τ_1	194ps	+ 113%
	τ_3	165ps	- 15%
	τ_5	147ps	- 39%

Memory is mainly related with the envelope response of the circuit. The expectation is the increase of the delay terms with respect to the increase of capacitance value. RC time constant arising from input bias network increases when dc block capacitance increases. Expectation is partly realized. As it is seen in the Table 4-13, τ_1 increases conspicuously depending on the increase of capacitance; however τ_3 decreases a little amount and τ_5 decreases more than 35%.

In the second case, inductor of input bias circuit L1 is changed from 6.2nH to 27nH. Table 4-14 presents delay terms and variations of delay terms with respect to initial values.

Table 4-14: Coefficients and Delay Terms of Case-2

L1			
Coefficients	a_1	4.571	
	a_3	-0.0059	
	a_5	0.00011	
Delay Terms	τ_1	204ps	+ 124%
	τ_3	165ps	- 15%
	τ_5	147ps	- 39%

Changing the choke inductor of input bias network changes the impedance seen at the gate terminal of the transistor at low frequencies. Thus, delay terms vary.

According to the Table 4-14, τ_1 increases by 124% depending on the increase of inductance; τ_3 and τ_5 decrease. Results of Case-1 and Case-2 look similar.

In the third case, inductor of the output bias circuit is changed from 7,6nH to 27nH. Delay terms and variations of delay terms with respect to the initial values are listed in Table 4-15.

Table 4-15: Coefficients and Delay Terms of Case-3

L2			
Coefficients	a_1	4.571	
	a_3	-0.0059	
	a_5	0.00011	
Delay Terms	τ_1	191ps	+ 110%
	τ_3	171ps	- 12%
	τ_5	154ps	- 36%

It is seen that τ_1 increases conspicuously depending on the increase of inductance, τ_3 decreases by a little amount. Variation of τ_5 is bigger than the variation of τ_3.

Another measurement is performed to see how much delay terms vary as the value of bias circuit component varies. In Figure 4-10, capacitor of output bias circuit C3 is seen. In the original circuit, value of C3 is 6.8pF. For this experiment, C3 is changed to 15pF, 30pF and 56pF respectively and variation of delay terms are observed.

Table 4-16: Calculated Delay Terms at Different Output Bias Circuit Conditions

	6.8pF	15pF	30pF	56pF
τ_1	83ps	106ps	144ps	154ps
τ_3	105ps	168ps	225ps	251ps
τ_5	271ps	256ps	245ps	243ps

It is seen that two of the delay terms increase with respect to the increase of capacitance however, third delay term decreases. Figure 4-11 illustrates the variation of delay terms with respect to the capacitance value.

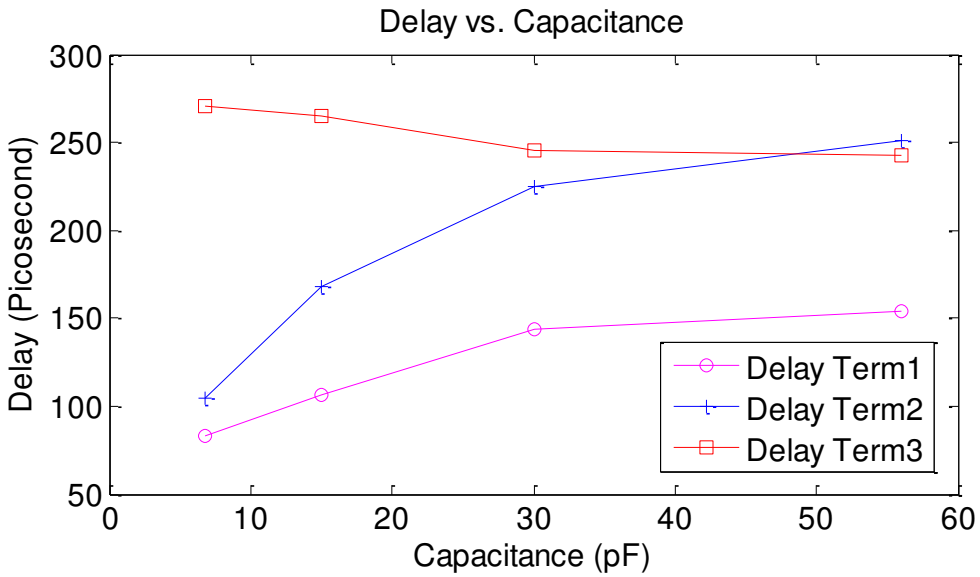

Figure 4-11 Variation of Delay Terms with Respect to the Capacitance Values

As expected, delay terms τ_1 and τ_3 increase with the increase of capacitance despite that delay term τ_5 decreases. Change of delay terms shows a trend; there are no peaks or dips seen in the variation.

Gathering the variation of delay terms with respect to the bias circuit components is important. It is essential to use choke inductors and dc block capacitances while designing a PA. Knowing the effect of inductors or capacitors on delay terms gives a

designer the opportunity to choose optimum values for circuit components which helps to minimize memory effect.

4.4 Tuning of Model Parameters

Tuning is an approach which is used to increase model accuracy. In literature, many approaches use tuning to achieve more accurate model parameters. It is declared before that NMSE is a practical criterion to measure/check model validity. In this section, results of tuning which is carried out to improve modeling accuracy are presented.

Tuning is done by monitoring the NMSE which is calculated with the equation using measured time domain output signal and simulated time domain output signal. Tuning is run for 4 different cases in which capacitance of output bias circuit C3 is 6.8pF, 15pF, 30pF and 56pF respectively.

Table 4-17: Tuning of Model Parameters for the Case in Which C3 is 6.8pF

1. Cycle	NMSE	2. Cycle	NMSE	3. Cycle	NMSE
τ1 = 340ps	-5,82	τ1 = 290ps	-15,23	τ1 = 290ps	-15,23
τ3 = 340ps		τ3 = 340ps		τ3 = 320ps	
τ5 = 340ps		τ5 = 340ps		τ5 = 340ps	
τ1 = 290ps	-15,23	τ1 = 290ps	-15,23	τ1 = 290ps	-15,17
τ3 = 340ps		τ3 = 320ps		τ3 = 320ps	
τ5 = 340ps		τ5 = 340ps		τ5 = 320ps	
τ1 = 270ps	-11,88	τ1 = 290ps	-14,84	τ1 = 290ps	-15,21
τ3 = 340ps		τ3 = 300ps		τ3 = 320ps	
τ5 = 340ps		τ5 = 340ps		τ5 = 330ps	
τ1 = 310ps	-11,63				
τ3 = 340ps					
τ5 = 340ps					
τ1 = 300ps	-13,97				
τ3 = 340ps					
τ5 = 340ps					
τ1 = 280ps	-14,17				
τ3 = 340ps					
τ5 = 340ps					

C = 6.8pF	
a1	4,07
a3	-0,006
a5	0,00012
	NMSE
τ1 = 290ps	-15,23
τ3 = 320ps	
τ5 = 340ps	

Sampling time interval of the time domain input signal is 80ps. Sampling time interval determines the resolution of the tuning. To heal the resolution interpolation is used in MATLAB. Interpolation increases the data size without deteriorating the

signal. The data size is increased to the 8 times of original data size and the new resolution for tuning is 10ps.

In the first cycle, optimum value for delay term τ_1 is investigated. After achieving the optimum for τ_1 second and third cycles are carried out to find the optimums for delay terms τ_3 and τ_5. Tuning is also applied to the model coefficients a_1, a_3 and a_5. Optimums for these coefficients are also given in Table 4-17.

Table 4-18: Tuning of Model Parameters for the Case in Which C3 is 15pF

1. Cycle	NMSE	2. Cycle	NMSE	3. Cycle	NMSE		C = 15pF	
τ1 = 340ps	-9,54	τ1 = 310ps	-16,14	τ1 = 310ps	-16,14			
τ3 = 340ps		τ3 = 340ps		τ3 = 330ps			a1	4,07
τ5 = 340ps		τ5 = 340ps		τ5 = 340ps			a3	-0,006
τ1 = 310ps	-16,14	τ1 = 310ps	-15,76	τ1 = 310ps	-15,95		a5	0,00012
τ3 = 340ps		τ3 = 310ps		τ3 = 330ps				
τ5 = 340ps		τ5 = 340ps		τ5 = 310ps				NMSE
τ1 = 280ps	-10,1	τ1 = 310ps	-14,68	τ1 = 310ps	-15,66		τ1 = 310ps	-16,14
τ3 = 340ps		τ3 = 280ps		τ3 = 330ps			τ3 = 330ps	
τ5 = 340ps		τ5 = 340ps		τ5 = 280ps			τ5 = 340ps	
τ1 = 250ps	-4,89	τ1 = 310ps	-16,14					
τ3 = 340ps		τ3 = 330ps						
τ5 = 340ps		τ5 = 340ps						
τ1 = 300ps	-15,08	τ1 = 310ps	-16					
τ3 = 340ps		τ3 = 320ps						
τ5 = 340ps		τ5 = 340ps						
τ1 = 320ps	-14,5							
τ3 = 340ps								
τ5 = 340ps								

Table 4-18 presents the steps of tuning approach for the case in which C3 is 15pF. Three cycles are run one after the other to achieve the best NMSE value. Delay terms which produce the best NMSE are marked with yellow color. Best value of NMSE is calculated as -16,14dB. It is seen that the significant factor affecting NMSE is the delay term τ_1. Change of delay terms τ_3 and τ_5 don't affect the NMSE critically.

Table 4-19: Tuning of Model Parameters for the Case in Which C3 is 30pF

1. Cycle	NMSE	2. Cycle	NMSE	3. Cycle	NMSE
τ1 = 340ps	-11,97	τ1 = 320ps	-16,34	τ1 = 320ps	-16,34
τ3 = 340ps		τ3 = 340ps		τ3 = 340ps	
τ5 = 340ps		τ5 = 340ps		τ5 = 340ps	
τ1 = 310ps	-15,24	τ1 = 320ps	-15,88	τ1 = 320ps	-16,04
τ3 = 340ps		τ3 = 310ps		τ3 = 340ps	
τ5 = 340ps		τ5 = 340ps		τ5 = 310ps	
τ1 = 280ps	-8,07	τ1 = 320ps	-16,15	τ1 = 320ps	-16,14
τ3 = 340ps		τ3 = 320ps		τ3 = 340ps	
τ5 = 340ps		τ5 = 340ps		τ5 = 320ps	
τ1 = 250ps	-3,65	τ1 = 320ps	-16,31	τ1 = 320ps	-16,24
τ3 = 340ps		τ3 = 330ps		τ3 = 340ps	
τ5 = 340ps		τ5 = 340ps		τ5 = 330ps	
τ1 = 300ps	-12,63				
τ3 = 340ps					
τ5 = 340ps					
τ1 = 320ps	-16,34				
τ3 = 340ps					
τ5 = 340ps					
τ1 = 330ps	-14,62				
τ3 = 340ps					
τ5 = 340ps					

C = 30pF	
a1	4,07
a3	-0,006
a5	0,00012
	NMSE
τ1 = 320ps	-16,34
τ3 = 340ps	
τ5 = 340ps	

Results of tuning for the case in which C3 is 30pF are presented in Table 4-19. The best value of NMSE is -16,34 dB which is close to the result of the previous condition. Again it is observed that delay term τ_1 is the significant factor affecting the NMSE. Variations of other delay terms don't affect NMSE significantly.

Table 4-20: Tuning of Model Parameters for the Case in Which C3 is 56pF

1. Cycle	NMSE	2. Cycle	NMSE	3. Cycle	NMSE		C = 56pF	
τ1 = 340ps	-13,14	τ1 = 320ps	-15,27	τ1 = 320ps	-15,41			
τ3 = 340ps		τ3 = 340ps		τ3 = 320ps			a1	4,07
τ5 = 340ps		τ5 = 340ps		τ5 = 340ps			a3	-0,006
τ1 = 290ps	-8,62	τ1 = 320ps	-15,41	τ1 = 320ps	-15,15		a5	0,00012
τ3 = 340ps		τ3 = 320ps		τ3 = 320ps				
τ5 = 340ps		τ5 = 340ps		τ5 = 320ps				NMSE
τ1 = 320ps	-15,27	τ1 = 320ps	-15,12	τ1 = 320ps	-15,27		τ1 = 320ps	-15,41
τ3 = 340ps		τ3 = 300ps		τ3 = 320ps			τ3 = 320ps	
τ5 = 340ps		τ5 = 340ps		τ5 = 330ps			τ5 = 340ps	
τ1 = 330ps	-15,23	τ1 = 320ps	-15,4					
τ3 = 340ps		τ3 = 330ps						
τ5 = 340ps		τ5 = 340ps						
τ1 = 310ps	-13,22							
τ3 = 340ps								
τ5 = 340ps								

Best NMSE that is achieved for the last case is -15,41dB. Figure 4-12 shows the variation of tuned delay terms with respect to the capacitance values. It is seen that delay terms τ_1 and τ_3 increase with respect to the increase of capacitance however, delay term τ_5 doesn't change. Variation of tuned delay terms that are presented in Figure 4-12 is similar with the variation of original delay terms which are presented in Figure 4-11. This means that NMSE based tuning approach doesn't change the general behavior of the delay terms with respect to the capacitance values.

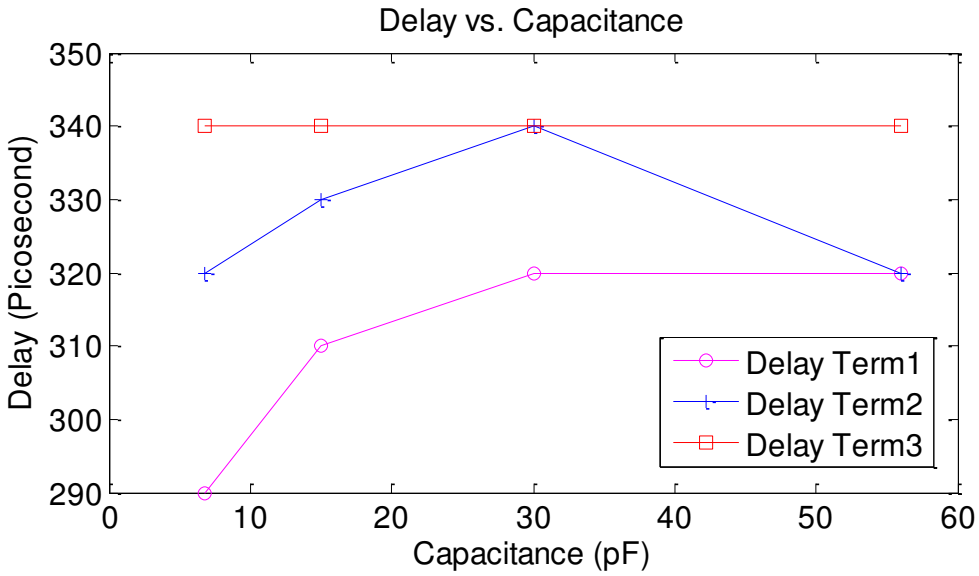

Figure 4-12 Variation of Tuned Delay Terms with Respect to the Capacitance Values

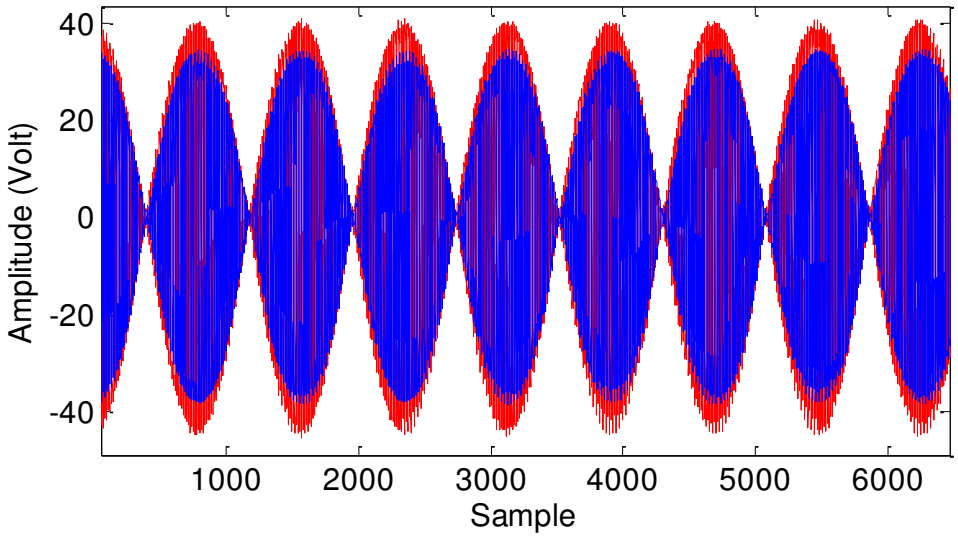

Figure 4-13 Measured Time Domain Output Signal (blue) and Simulated Time Domain Output Signal (red) Produced with the Initial Model Parameters

Figure 4-13 shows measured time domain output signal and simulated time domain output signal. Simulated signal is produced with the initial model parameters. A time shift is easily seen in the figure.

Figure 4-14 presents measured time domain output signal and simulated time domain output signal which is produced with the tuned model parameters. Time shift doesn't

exist in Figure 4-14. Difference between amplitudes of measured and simulated signal is smaller in Figure 4-14 comparing with the difference in Figure 4-13.

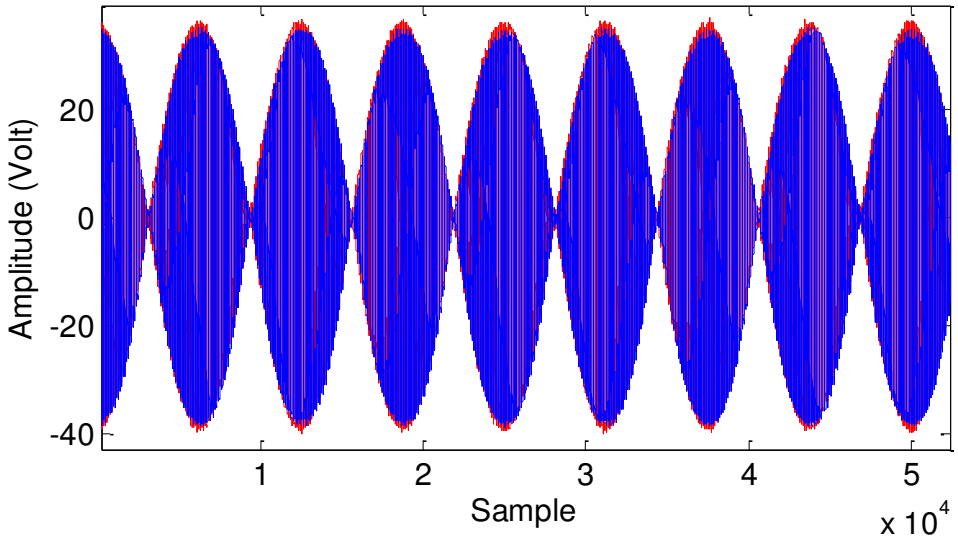

Figure 4-14 Measured Time Domain Output Signal (blue) and Simulated Time Domain Output Signal (red) Produced with the Tuned Model Parameters

Figure 4-14 proves that tuning model parameters improves modeling capability; it is one of the most important outcomes of this study. This study declares that it is possible to analytically calculate delay terms and initial delay terms which are achieved can be tuned to improve modeling capability.

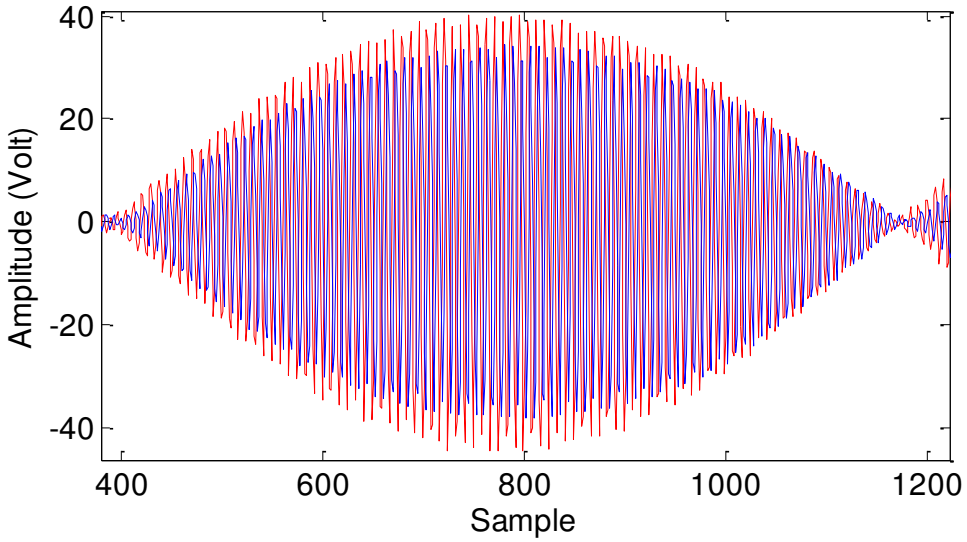

Figure 4-15 One Cycle of the Envelope of Measured Time Domain Output Signal (blue) and Simulated Time Domain Output Signal (red) Produced with the Initial Model Parameters

Figure 4-15 shows one cycle of the envelope of measured time domain output signal and simulated time domain output signal which is produced with the initial model parameters. RF signals which fill inside of the envelopes are seen in the figure. RF signal inside the envelope of simulated time domain output signal follows the RF signal inside the envelope of measured time domain output signal with a little shift.

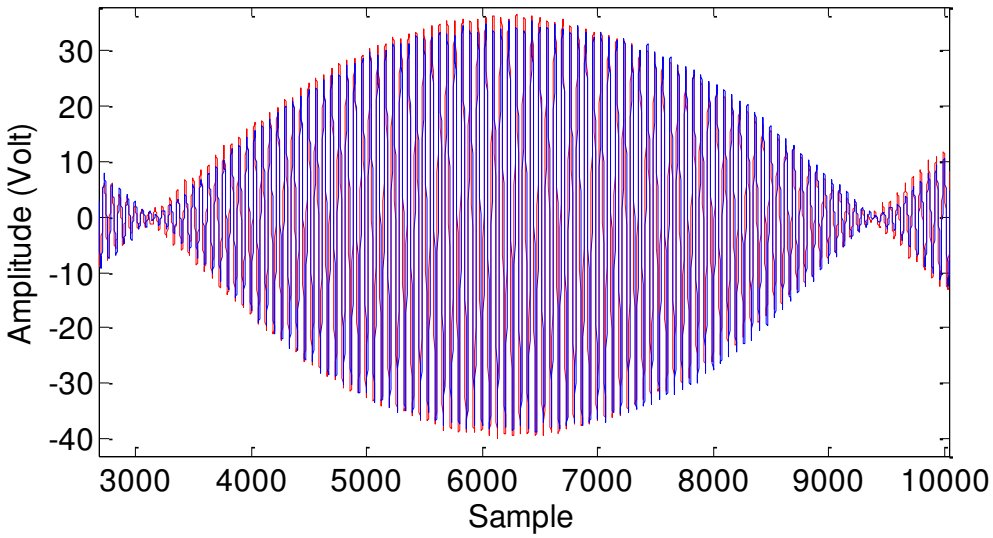

Figure 4-16 One Cycle of the Envelope of Measured Time Domain Output Signal (blue) and Simulated Time Domain Output Signal (red) Produced with the Tuned Model Parameters

Figure 4-16 shows one cycle of the envelope of measured time domain output signal and simulated time domain output signal which is produced with the tuned model parameters. RF signals which fill inside of the envelopes are seen in the figure. RF signal inside the envelope of simulated time domain output signal follows the RF signal inside the envelope of measured time domain output signal with a little shift.

This shift is smaller than the shift seen in the Figure 4-15. This means that tuning improves modeling capability. Both RF signal and envelope signal are modeled close to real.

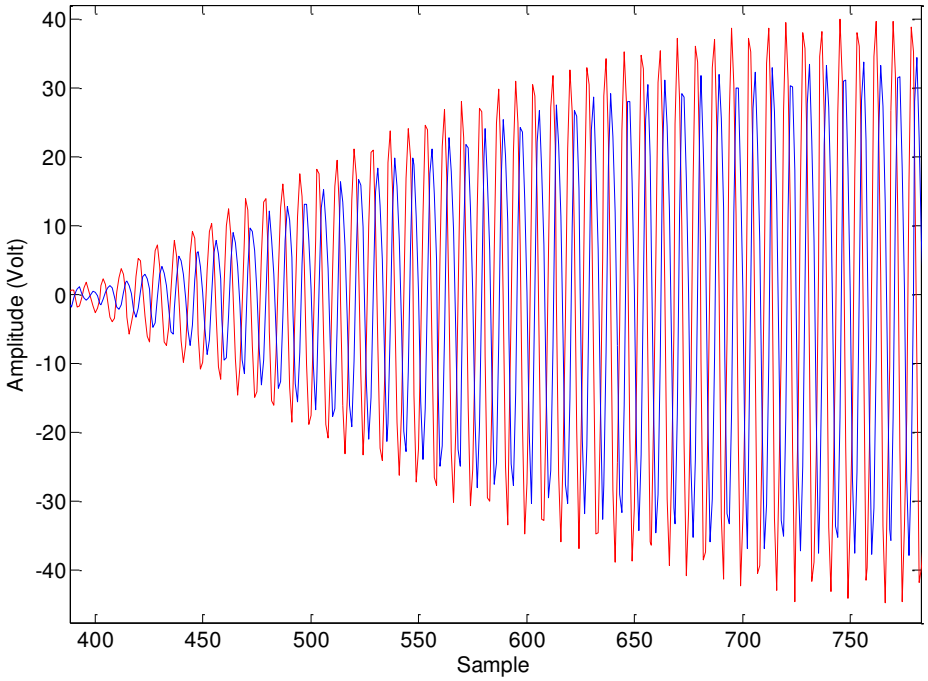

Figure 4-17 Half Cycle of the Envelope of Measured Time Domain Output Signal (blue) and Simulated Time Domain Output Signal (red) Produced with the Initial Model Parameters

Figure 4-17 shows the half cycle of the envelope of measured time domain output signal and simulated time domain output signal which is produced with the initial model parameters. There is a shift seen between RF signals.

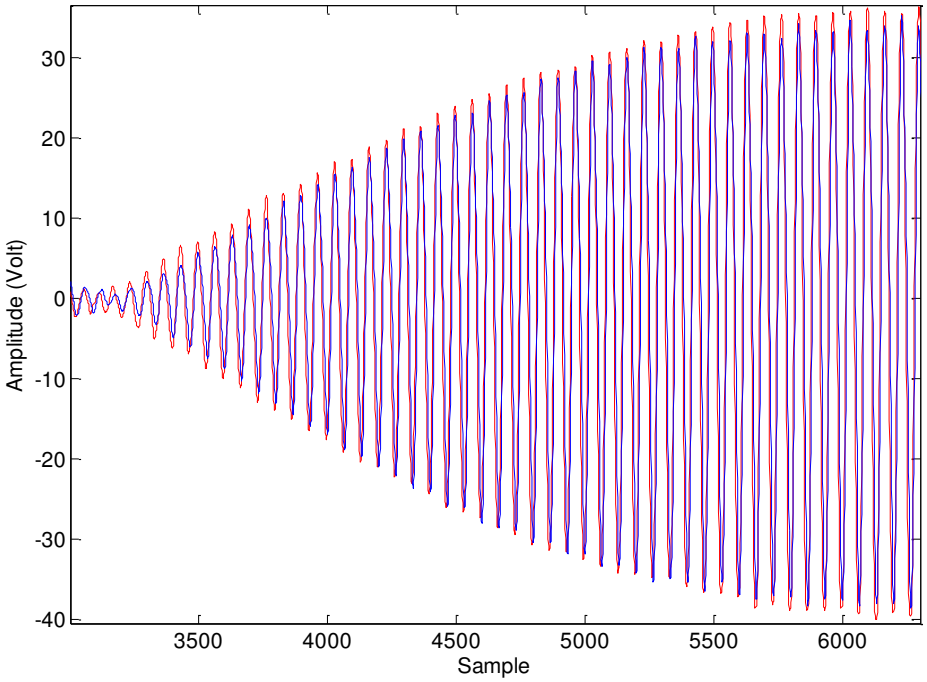

Figure 4-18 Half Cycle of the Envelope of Measured Time Domain Output Signal (blue) and Simulated Time Domain Output Signal (red) Produced with the Tuned Model Parameters

Figure 4-18 shows the half cycle of the envelope of measured time domain output signal and simulated time domain output signal which is produced with the tuned model parameters. It is seen that RF signal which fills inside the envelope of simulated time domain output signal follows the RF signal which fills inside the envelope of measured time domain output signal. RF signals are almost same. These figures prove that tuning increases modeling capability.

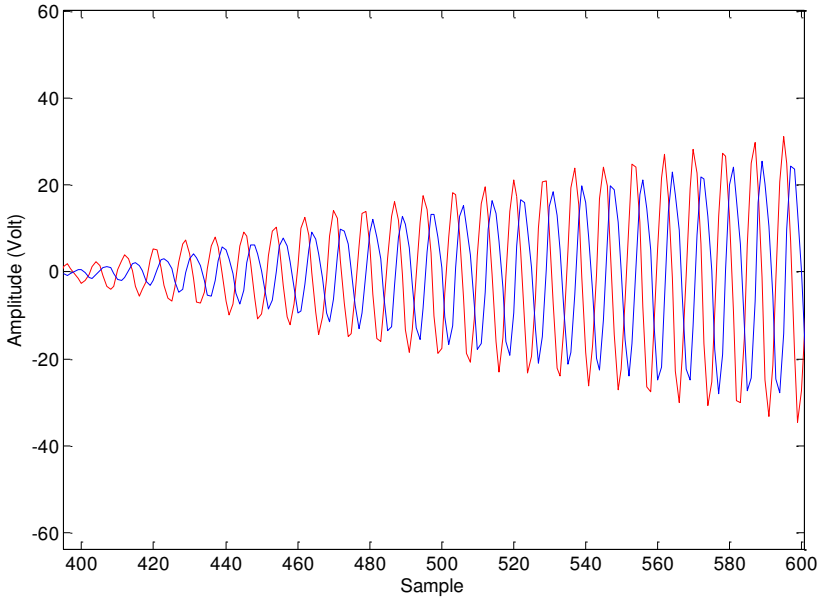

Figure 4-19 Quarter Cycle of the Envelope of Measured Time Domain Output Signal (blue) and Simulated Time Domain Output Signal (red) Produced with the Initial Model Parameters

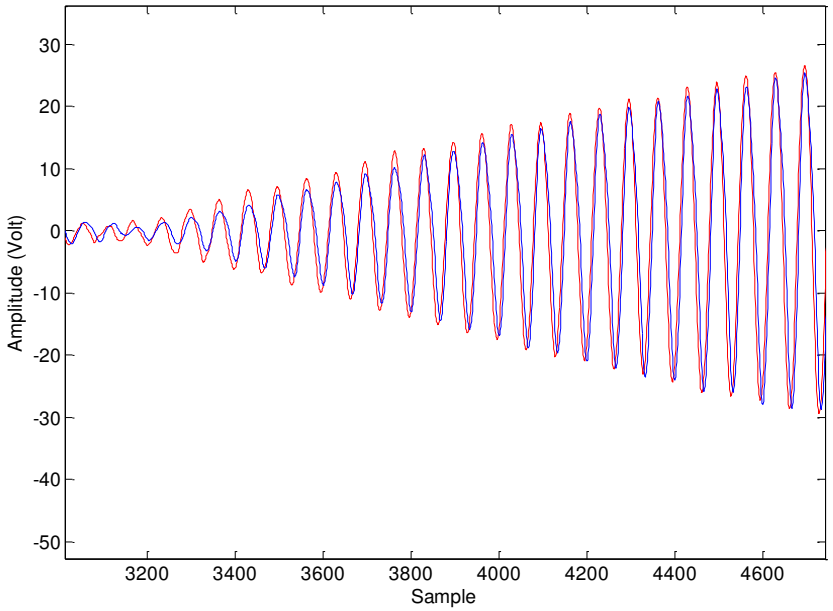

Figure 4-20 Quarter Cycle of the Envelope of Measured Time Domain Output Signal (blue) and Simulated Time Domain Output Signal (red) Produced with the Tuned Model Parameters

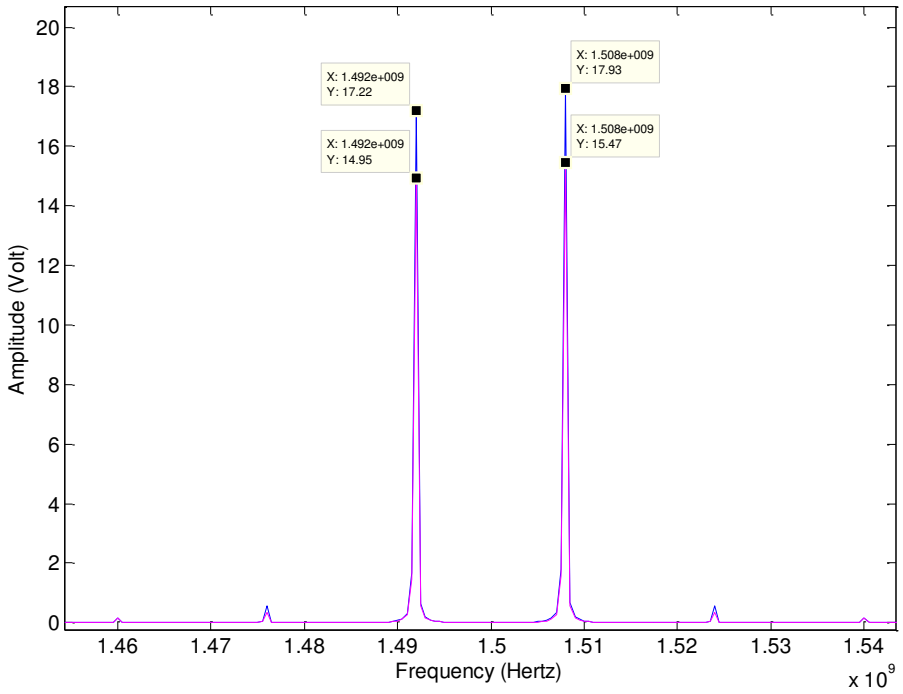

Figure 4-21 Simulated Frequency Domain Output Signal (blue) and Measured Frequency Domain Output Signal (magenta) Produced with the Initial Model Parameters

Simulated frequency domain output signal and measured frequency domain output signal which is produced with the initial model parameters are seen in Figure 4-21. Simulated signal and measured signal are similar. Error on the amplitude of single fundamental tone can be calculated as (17.22 – 14.95) / 14.95 = 0.15 → 15%.

Simulated frequency domain output signal and measured frequency domain output signal which is produced with the tuned model parameters are seen in Figure 4-22. Error on the amplitude of single fundamental tone can be calculated as

(13.97 -12.96) / 12.96 = 0.08 → 8%.

Error is smaller on the simulated signal which is produced with tuned model parameters comparing with the error on the simulated signal which is produced with initial model parameters.

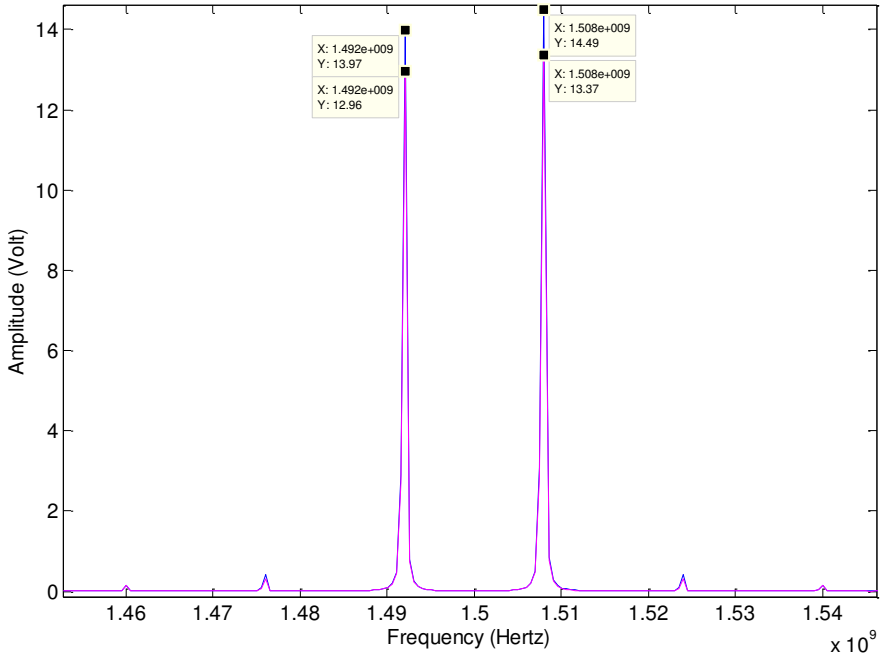

Figure 4-22 Simulated Frequency Domain Output Signal (blue) and Measured Frequency Domain Output Signal (magenta) Produced with the Tuned Model Parameters

In this chapter, results of the measurements and outcomes of the model construction approach are presented. Validity of the model is tested by using NMSE. Tuning approach is introduced which is applied to the initial values of calculated model parameters to increase modeling achievement. Usefulness of the approach is proved and presented with illustrations. Simulated and measured output signals are compared both in RF case and in envelope case.

CHAPTER 5

CONCLUSION & FUTURE WORK

In this study, memory of a PA is investigated. A 5^{th} order polynomial that exhibits memory is used to model a 1-2GHz 10W output power class AB power amplifier. A convenient measurement setup is built to collect required waveforms and a novel method is developed to identify parameters of the polynomial.

Relationship between excitation signal bandwidth and delay terms is investigated by performing measurements with increasing input signal bandwidth. Also interaction between bias circuit components and delay terms are enlightened. Effects of change of inductances and capacitors on delay terms are shown with tables. Variation of delay terms with respect to the different capacitances that are used in the output bias network is presented. A meaningful trend is discovered in this variation.

Success of modeling approach is examined with a criterion called NMSE which is generally used for testing modeling success. Tuning is applied to the initial values of coefficients and delay terms to decrease NMSE and increase model accuracy. After tuning, variation of tuned delay terms with respect to the different capacitances that are used in the output bias network is investigated. Variation is similar with the variation which is discovered for the delay terms that are not tuned.

This study is special because model parameters -delay terms and coefficients- are declared which haven't been declared before. Also, relationship between bias circuit components and delay terms are shown with graphs. A quite good modeling success is achieved.

It is known that power of excitation signal is effective on delay terms; as a future work, measurements can be performed to observe the variation of delay terms with respect to the input power level.

In this study, even order terms weren't taken into account in the model polynomial; a new model which contains both even order terms and odd order terms can be used to model PA nonlinearity and memory more precisely. However, this model can be a complex one which causes more complex mathematical expressions to solve while achieving the parameters of the polynomial. The approach can decrease NMSE and increase model accuracy. While performing measurements, increasing sampling rate and data length is useful for reaching more accurate model parameters.

REFERENCES

[1] Yan Ye, Taijun Liu, Tiefeng Xu and F. M. Ghannouchi, "Analysis and Decomposition of the Nonlinearities in RF Power Amplifiers," in 6th International Conference on Wireless Communications Networking and Mobile Computing (WiCOM), 23-25 Sept. 2010, Chengdu, pp.1-4.

[2] Hyunchul Ku, J. S. Kenney, "Behavioral Modeling of Nonlinear RF Power Amplifiers Considering Memory Effects," IEEE Transactions on Microwave Theory and Techniques, Vol.51, No.12, pp.2495-2504, 2003.

[3] F. M. Ghannouchi and O. Hammi, "Behavioral Modeling and Predistortion," IEEE Microwave Magazine, Vol.10, No.7, pp.52-64, 2009.

[4] J. S. Kenney and P. Fedorenko, "Identification of RF Power Amplifier Memory Effect Origins using Third-Order Intermodulation Distortion Amplitude and Phase Asymmetry," in IEEE MTT-S International Microwave Symposium Digest, San Francisco, CA, 11-16 June 2006, pp.1121-1124.

[5] J. C. Pedro, J. C. Madaleno and J. A. Garcia, "Theoretical Basis for Extraction of Mildly Nonlinear Behavioral Models," Int. J. RF and Microwave CAE, Vol.13, No.1, pp.40-53, 2003.

[6] D. Schreurs, M. O'Droma, A. A. Goacher and M. Gadringer, "RF Power Amplifier Behavioral Modeling," New York: Cambridge University Press, 2009.

[7] J. Vuolevi, T. Rahkonen and J. Manninen, "Measurement Technique for Characterizing Memory Effects in RF Power Amplifiers," IEEE Transactions on Microwave Theory and Techniques, Vol.49, No.8, pp.1383-1389, 2001.

[8] H. Wang, J. Bao and Z. Wu, "Comparison of the Behavioral Modelings for RF Power Amplifier With Memory Effects," IEEE Microwave and Wireless Components Letters, Vol.19, No.3, pp.179-181, 2009.

[9] J. Vuolevi and T. Rahkonen, "Distortion in RF Power Amplifiers," Massachusetts: Artech House, 2003.

[10] M. Golio and J. Golio, "RF and Microwave Circuits, Measurements, and Modeling," Florida: CRC Press, 2008.

[11] A. H. Yüzer, "Modeling of Asymmetric Intermodulation Distortion and Memory Effects of Power Amplifiers," Ph. D. Dissertation, Dept. of Electrical and Electronics Eng., METU, Ankara, Turkey 2011.

[12] Y. Oishi, S. Kimura, E. Fukuda, T. Takano, D. Takago, Y. Daido and K. Araki, "Design of Predistorter Using Measured Nonlinear Characteristics of Power Amplifier with Memory Effect," in IEEE 75th Vehicular Technology Conference, 6-9 May 2012, Yokohama, pp.1-5.

[13] A. H. Yüzer and Ş. Demir, "Behavioral Modeling of Asymmetric Intermodulation Distortion of Nonlinear Amplifier", in Progress in Electromagnetics Research Symposium, Cambridge, July 2010, pp.115-119.

[14] A. Mutlu, "Multi-Tone Representation of Arbitrary Waveforms and Application to the Analysis of Nonlinear Amplifiers and Feedforward Linearizers," M. Sc. Dissertation, Dept. of Electrical and Electronics Eng., METU, Ankara, Turkey 2005.

APPENDIX

Table A-1: Amplitude/Phase of Frequency Components of Measured Input Signal and Measured Output Signal for Measurement-1B

2MHz										
Input Signal				Output Signal						
Fundamentals				Fundamentals and Intermodulations						
	Frequency (MHz)	Amplitude (V)	Phase (°)		Frequency (MHz)	Amplitude (V)	Phase (°)			
f1	1499	4,9400	139,1	f1	1499	19,3100	-50,2			
f2	1501	4,8700	121,5	f2	1501	19,0300	-68,6			
				2f1-f2	1497	0,5530	148,6			
				2f2-f1	1503	0,5200	96,9	a5		
				3f1-2f2	1495	0,2210	168,6	3f1-2f2	0,00012	Average
				3f2-2f1	1505	0,2120	70,6	3f2-2f1	0,00012	0,00012

In Table A-1, amplitude/phase of frequency components of measured input signal and measured output signal for Measurement-1B are shown. This data is similar to the data achieved in Measurement-1A which is listed in Table 4-3.

Table A-2: Amplitude/Phase of Frequency Components of Measured Output Signal for Measurement-1B

2MHz						
Frequency	Amplitude (V)	Phase Expression (radian)	Phase Expression (°)	Amplitude (V)	Phase (radian)	Phase (°)
ω1	22,32	(-2π*f1)*(τ1)	-f1*(τ1)*360	19,310	-0,88	-50,20
	-1,41	(-2π*f1)*(τ3)	-f1*(τ3)*360			
	2,13	(-2π*f1)*(τ5)	-f1*(τ5)*360			
ω2	22,01	(-2π*f2)*(τ1)+φ	[((-2π*f2)*(τ1)+φ)/π]*180	19,030	-1,20	-68,60
	-1,40	(-2π*f2)*(τ3)+φ	[((-2π*f2)*(τ3)+φ)/π]*180			
	2,13	(-2π*f2)*(τ5)+φ	[((-2π*f2)*(τ5)+φ)/π]*180			
2ω1-ω2	-0,47	(-2π*(2f1-f2))*(τ3)-φ	[((-2π*(2f1-f2))*(τ3)-φ)/π]*180	0,553	2,59	148,60
	1,07	(-2π*(2f1-f2))*(τ5)-φ	[((-2π*(2f1-f2))*(τ5)-φ)/π]*180			
2ω2-ω1	-0,47	(-2π*(2f2-f1))*(τ3)+2φ	[((-2π*(2f2-f1))*(τ3)+2φ)/π]*180	0,520	1,69	96,90
	1,06	(-2π*(2f2-f1))*(τ5)+2φ	[((-2π*(2f2-f1))*(τ5)+2φ)/π]*180			
3ω1-2ω2	0,21	(-2π*(3f1-2f2))*(τ5)-2φ	[((-2π*(3f1-2f2))*(τ5)-2φ)/π]*180	0,221	2,94	168,60
3ω2-2ω1	0,21	(-2π*(3f2-2f1))*(τ5)+3φ	[((-2π*(3f2-2f1))*(τ5)+3φ)/π]*180	0,212	1,23	70,60

Table A-2 shows amplitude/phase of frequency components of measured output signal for Measurement-1B. Data seen is similar to the one listed in Table 4-4; this means measurements and calculations are consistent.

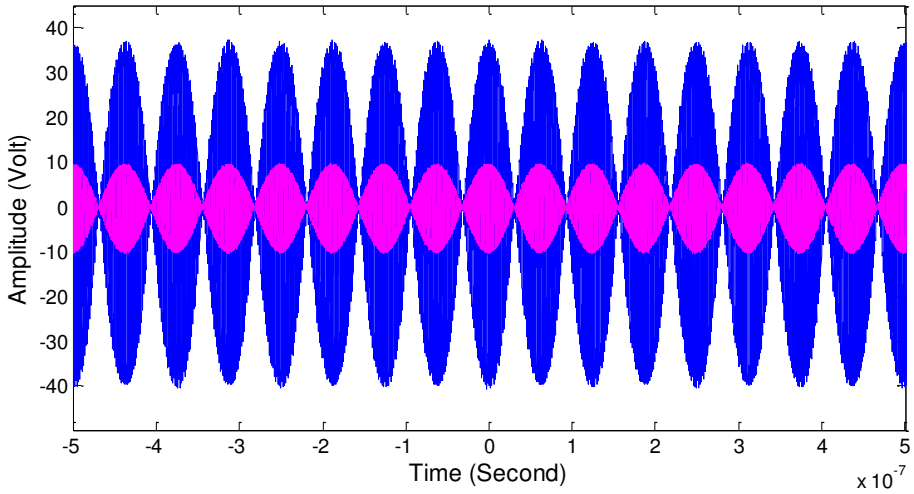

Figure A-1 Measured Time Domain Input Signal (magenta) and Measured Time Domain Output Signal (blue) for Measurement-2

Figure A-1 presents measured time domain input signal and measured time domain output signal for Measurement-2.

Table A-3: Amplitude/Phase of Frequency Components of Measured Input Signal and Measured Output Signal for Measurement-2

16MHz										
Input Signal				Output Signal						
Fundamentals				Fundamentals and Intermodulations						
	Frequency (MHz)	Amplitude (V)	Phase (°)		Frequency (MHz)	Amplitude (V)	Phase (°)			
f1	1492	4,8700	127,8	f1	1492	18,9100	-59,3			
f2	1508	5,0700	134,6	f2	1508	19,5800	-58,1			
				2f1-f2	1476	0,5630	114,3			
				2f2-f1	1524	0,5200	133,0	a5		
				3f1-2f2	1460	0,1880	125,2	3f1-2f2	0,0001	Average
				3f2-2f1	1540	0,2290	118,1	3f2-2f1	0,00012	0,00011

Table A-3 shows amplitude/phase of frequency components of measured input signal and measured output signal for Measurement-2. Table also shows coefficients a_5 calculated with two separate equations.

Table A-4: Amplitude/Phase of Frequency Components of Measured Output Signal for Measurement-2

16MHz						
Frequency	Amplitude (V)	Phase Expression (radian)	Phase Expression (°)	Amplitude (V)	Phase (radian)	Phase (°)
ω1	22,26	(-2π*f1)*(τ1)	-f1*(τ1)*360	18,910	-1,03	-59,30
	-1,62	(-2π*f1)*(τ3)	-f1*(τ3)*360			
	2,08	(-2π*f1)*(τ5)	-f1*(τ5)*360			
ω2	23,17	(-2π*f2)*(τ1)+φ	[((-2π*f2)*(τ1)+φ)/π]*180	19,580	-1,01	-58,10
	-1,64	(-2π*f2)*(τ3)+φ	[((-2π*f2)*(τ3)+φ)/π]*180			
	2,09	(-2π*f2)*(τ5)+φ	[((-2π*f2)*(τ5)+φ)/π]*180			
2ω1-ω2	-0,53	(-2π*(2f1-f2))*(τ3)-φ	[((-2π*(2f1-f2))*(τ3)-φ)/π]*180	0,563	1,99	114,30
	1,03	(-2π*(2f1-f2))*(τ5)-φ	[((-2π*(2f1-f2))*(τ5)-φ)/π]*180			
2ω2-ω1	-0,55	(-2π*(2f2-f1))*(τ3)+2φ	[((-2π*(2f2-f1))*(τ3)+2φ)/π]*180	0,520	2,32	133,00
	1,05	(-2π*(2f2-f1))*(τ5)+2φ	[((-2π*(2f2-f1))*(τ5)+2φ)/π]*180			
3ω1-2ω2	0,20	(-2π*(3f1-2f2))*(τ5)-2φ	[((-2π*(3f1-2f2))*(τ5)-2φ)/π]*180	0,188	2,18	125,20
3ω2-2ω1	0,21	(-2π*(3f2-2f1))*(τ5)+3φ	[((-2π*(3f2-2f1))*(τ5)+3φ)/π]*180	0,229	2,06	118,10

Table A-4 shows amplitude/phase of frequency components of measured output signal for Measurement-2. Table also shows calculated amplitudes of terms that contribute to frequency components.

Table A-5: Amplitude/Phase of Frequency Components of Measured Input Signal and Measured Output Signal When the Capacitor C1 Has Changed

C1										
Input Signal				Output Signal						
Fundamentals				Fundamentals and Intermodulations						
	Frequency (MHz)	Amplitude (V)	Phase (°)		Frequency (MHz)	Amplitude (V)	Phase (°)			
f1	1492	4,7800	-49,6	f1	1492	17,5000	118,8			
f2	1508	5,0500	-54,3	f2	1508	18,3700	109,0			
				2f1-f2	1476	0,3930	-61,7			
				2f2-f1	1524	0,3670	-71,0	a5		
				3f1-2f2	1460	0,1580	-31,2	3f1-2f2	0,00009	Average
				3f2-2f1	1540	0,2010	-95,1	3f2-2f1	0,00011	0,00010

Table A-6: Amplitude/Phase of Frequency Components of Measured Output Signal When the Capacitor C1 Has Changed

C1						
Frequency	Amplitude (V)	Phase Expression (radian)	Phase Expression (°)	Amplitude (V)	Phase (radian)	Phase (°)
ω1	21,85	(-2π*f1)*(τ1)	-f1*(τ1)*360	17,500	2,07	118,80
	-1,56	(-2π*f1)*(τ3)	-f1*(τ3)*360			
	1,78	(-2π*f1)*(τ5)	-f1*(τ5)*360			
ω2	23,08	(-2π*f2)*(τ1)+φ	[((-2π*f2)*(τ1)+φ)/π]*180	18,370	1,90	109,00
	-1,59	(-2π*f2)*(τ3)+φ	[((-2π*f2)*(τ3)+φ)/π]*180			
	1,80	(-2π*f2)*(τ5)+φ	[((-2π*f2)*(τ5)+φ)/π]*180			
2ω1-ω2	-0,51	(-2π*(2f1-f2))*(τ3)-φ	[((-2π*(2f1-f2))*(τ3)-φ)/π]*180	0,393	-1,08	-61,70
	0,88	(-2π*(2f1-f2))*(τ5)-φ	[((-2π*(2f1-f2))*(τ5)-φ)/π]*180			
2ω2-ω1	-0,54	(-2π*(2f2-f1))*(τ3)+2φ	[((-2π*(2f2-f1))*(τ3)+2φ)/π]*180	0,367	-1,24	-71,00
	0,91	(-2π*(2f2-f1))*(τ5)+2φ	[((-2π*(2f2-f1))*(τ5)+2φ)/π]*180			
3ω1-2ω2	0,17	(-2π*(3f1-2f2))*(τ5)-2φ	[((-2π*(3f1-2f2))*(τ5)-2φ)/π]*180	0,158	-0,54	-31,20
3ω2-2ω1	0,18	(-2π*(3f2-2f1))*(τ5)+3φ	[((-2π*(3f2-2f1))*(τ5)+3φ)/π]*180	0,201	-1,66	-95,10

Table A-7: Amplitude/Phase of Frequency Components of Measured Input Signal and Measured Output Signal When the Inductor L1 Has Changed

L1										
Input Signal				Output Signal						
Fundamentals				Fundamentals and Intermodulations						
	Frequency (MHz)	Amplitude (V)	Phase (°)		Frequency (MHz)	Amplitude (V)	Phase (°)			
f1	1492	4,7800	-50,7	f1	1492	17,7600	121,4			
f2	1508	5,0300	-53,7	f2	1508	18,5900	113,1			
				2f1-f2	1476	0,3970	-59,9			
				2f2-f1	1524	0,3630	-63,4	a5		
				3f1-2f2	1460	0,1680	-31,1	3f1-2f2	0,0001	Average
				3f2-2f1	1540	0,2130	-91,6	3f2-2f1	0,00012	0,00011

Table A-8: Amplitude/Phase of Frequency Components of Measured Output Signal When the Inductor L1 Has Changed

L1						
Frequency	Amplitude (V)	Phase Expression (radian)	Phase Expression (°)	Amplitude (V)	Phase (radian)	Phase (°)
ω1	21,85	(-2π*f1)*(τ1)	-f1*(τ1)*360	17,760	2,12	121,40
	-1,55	(-2π*f1)*(τ3)	-f1*(τ3)*360			
	1,94	(-2π*f1)*(τ5)	-f1*(τ5)*360			
ω2	22,99	(-2π*f2)*(τ1)+φ	[((-2π*f2)*(τ1)+φ)/π]*180	18,590	1,97	113,10
	-1,58	(-2π*f2)*(τ3)+φ	[((-2π*f2)*(τ3)+φ)/π]*180			
	1,96	(-2π*f2)*(τ5)+φ	[((-2π*f2)*(τ5)+φ)/π]*180			
2ω1-ω2	-0,51	(-2π*(2f1-f2))*(τ3)-φ	[((-2π*(2f1-f2))*(τ3)-φ)/π]*180	0,397	-1,04	-59,90
	0,96	(-2π*(2f1-f2))*(τ5)-φ	[((-2π*(2f1-f2))*(τ5)-φ)/π]*180			
2ω2-ω1	-0,54	(-2π*(2f2-f1))*(τ3)+2φ	[((-2π*(2f2-f1))*(τ3)+2φ)/π]*180	0,363	-1,11	-63,40
	0,99	(-2π*(2f2-f1))*(τ5)+2φ	[((-2π*(2f2-f1))*(τ5)+2φ)/π]*180			
3ω1-2ω2	0,19	(-2π*(3f1-2f2))*(τ5)-2φ	[((-2π*(3f1-2f2))*(τ5)-2φ)/π]*180	0,168	-0,54	-31,10
3ω2-2ω1	0,20	(-2π*(3f2-2f1))*(τ5)+3φ	[((-2π*(3f2-2f1))*(τ5)+3φ)/π]*180	0,213	-1,60	-91,60

Table A-9: Amplitude/Phase of Frequency Components of Measured Input Signal and Measured Output Signal When the Inductor L2 Has Changed

L2										
Input Signal				Output Signal						
Fundamentals				Fundamentals and Intermodulations						
	Frequency (MHz)	Amplitude (V)	Phase (°)		Frequency (MHz)	Amplitude (V)	Phase (°)			
f1	1492	4,7300	-50,2	f1	1492	17,6200	121,8			
f2	1508	5,0200	-56,7	f2	1508	18,6400	109,3			
				2f1-f2	1476	0,4070	-64,4			
				2f2-f1	1524	0,3710	-66,6	a5		
				3f1-2f2	1460	0,1540	-18,3	3f1-2f2	0,00009	Average
				3f2-2f1	1540	0,2100	-104,5	3f2-2f1	0,00012	0,00011

Table A-10: Amplitude/Phase of Frequency Components of Measured Output Signal When the Inductor L2 Has Changed

L2						
Frequency	Amplitude (V)	Phase Expression (radian)	Phase Expression (°)	Amplitude (V)	Phase (radian)	Phase (°)
ω1	21,62	(-2π*f1)*(τ1)	-f1*(τ1)*360	17,620	2,12	121,80
	-1,52	(-2π*f1)*(τ3)	-f1*(τ3)*360			
	1,88	(-2π*f1)*(τ5)	-f1*(τ5)*360			
ω2	22,95	(-2π*f2)*(τ1)+φ	[((-2π*f2)*(τ1)+φ)/π]*180	18,640	1,91	109,30
	-1,55	(-2π*f2)*(τ3)+φ	[((-2π*f2)*(τ3)+φ)/π]*180			
	1,90	(-2π*f2)*(τ5)+φ	[((-2π*f2)*(τ5)+φ)/π]*180			
2ω1-ω2	-0,50	(-2π*(2f1-f2))*(τ3)-φ	[((-2π*(2f1-f2))*(τ3)-φ)/π]*180	0,407	-1,12	-64,40
	0,93	(-2π*(2f1-f2))*(τ5)-φ	[((-2π*(2f1-f2))*(τ5)-φ)/π]*180			
2ω2-ω1	-0,53	(-2π*(2f2-f1))*(τ3)+2φ	[((-2π*(2f2-f1))*(τ3)+2φ)/π]*180	0,371	-1,16	-66,60
	0,96	(-2π*(2f2-f1))*(τ5)+2φ	[((-2π*(2f2-f1))*(τ5)+2φ)/π]*180			
3ω1-2ω2	0,18	(-2π*(3f1-2f2))*(τ5)-2φ	[((-2π*(3f1-2f2))*(τ5)-2φ)/π]*180	0,154	-0,32	-18,30
3ω2-2ω1	0,19	(-2π*(3f2-2f1))*(τ5)+3φ	[((-2π*(3f2-2f1))*(τ5)+3φ)/π]*180	0,210	-1,82	-104,50

Table A-11: Amplitude/Phase of Frequency Components of Measured Input Signal and Measured Output Signal When the Capacitor C3 is 6.8pF

16MHz - 6.8pF										
Input Signal				Output Signal						
Fundamentals				Fundamentals and Intermodulations						
	Frequency (MHz)	Amplitude (V)	Phase (°)		Frequency (MHz)	Amplitude (V)	Phase (°)			
f1	1492	4,7700	-55,0	f1	1492	18,0900	150,9			
f2	1508	4,9900	-55,0	f2	1508	18,7900	146,0			
				2f1-f2	1476	0,4293	-27,3			
				2f2-f1	1524	0,4399	-26,7	a5		
				3f1-2f2	1460	0,1855	-8,3	3f1-2f2	0,00011	Average
				3f2-2f1	1540	0,2131	-45,9	3f2-2f1	0,00012	0,00012

Table A-12: Amplitude/Phase of Frequency Components of Measured Output Signal When the Capacitor C3 is 6.8pF

16MHz-6,8pF						
Frequency	Amplitude (V)	Phase Expression (radian)	Phase Expression (°)	Amplitude (V)	Phase (radian)	Phase (°)
ω1	21,80	(-2π*f1)*(τ1)	-f1*(τ1)*360	18,090	2,63	150,90
	-1,53	(-2π*f1)*(τ3)	-f1*(τ3)*360			
	2,07	(-2π*f1)*(τ5)	-f1*(τ5)*360			
ω2	22,81	(-2π*f2)*(τ1)+φ	[((-2π*f2)*(τ1)+φ)/π]*180	18,790	2,55	146,00
	-1,55	(-2π*f2)*(τ3)+φ	[((-2π*f2)*(τ3)+φ)/π]*180			
	2,09	(-2π*f2)*(τ5)+φ	[((-2π*f2)*(τ5)+φ)/π]*180			
2ω1-ω2	-0,50	(-2π*(2f1-f2))*(τ3)-φ	[((-2π*(2f1-f2))*(τ3)-φ)/π]*180	0,429	-0,48	-27,30
	1,02	(-2π*(2f1-f2))*(τ5)-φ	[((-2π*(2f1-f2))*(τ5)-φ)/π]*180			
2ω2-ω1	-0,53	(-2π*(2f2-f1))*(τ3)+2φ	[((-2π*(2f2-f1))*(τ3)+2φ)/π]*180	0,440	-0,47	-26,70
	1,05	(-2π*(2f2-f1))*(τ5)+2φ	[((-2π*(2f2-f1))*(τ5)+2φ)/π]*180			
3ω1-2ω2	0,20	(-2π*(3f1-2f2))*(τ5)-2φ	[((-2π*(3f1-2f2))*(τ5)-2φ)/π]*180	0,186	-0,14	-8,30
3ω2-2ω1	0,21	(-2π*(3f2-2f1))*(τ5)+3φ	[((-2π*(3f2-2f1))*(τ5)+3φ)/π]*180	0,213	-0,80	-45,90

Table A-13: Amplitude/Phase of Frequency Components of Measured Input Signal and Measured Output Signal When the Capacitor C3 is 15pF

16MHz - 15pF										
Input Signal				Output Signal						
Fundamentals				Fundamentals and Intermodulations						
	Frequency (MHz)	Amplitude (V)	Phase (°)		Frequency (MHz)	Amplitude (V)	Phase (°)			
f1	1492	4,7800	-47,2	f1	1492	18,7000	148,5			
f2	1508	5,0300	-49,9	f2	1508	19,5000	140,8			
				2f1-f2	1476	0,6965	-14,5			
				2f2-f1	1524	0,7467	-27,7	a5		
				3f1-2f2	1460	0,2160	-18,8	3f1-2f2	0,00013	Average
				3f2-2f1	1540	0,2792	-67,7	3f2-2f1	0,00015	0,00014

Table A-14: Amplitude/Phase of Frequency Components of Measured Output Signal When the Capacitor C3 is 15pF

16MHz-15pF						
Frequency	Amplitude (V)	Phase Expression (radian)	Phase Expression (°)	Amplitude (V)	Phase (radian)	Phase (°)
ω1	21,85	(-2π*f1)*(τ1)	-f1*(τ1)*360	18,700	2,59	148,50
	-1,55	(-2π*f1)*(τ3)	-f1*(τ3)*360			
	2,47	(-2π*f1)*(τ5)	-f1*(τ5)*360			
ω2	22,99	(-2π*f2)*(τ1)+φ	[((-2π*f2)*(τ1)+φ)/π]*180	19,500	2,46	140,80
	-1,58	(-2π*f2)*(τ3)+φ	[((-2π*f2)*(τ3)+φ)/π]*180			
	2,50	(-2π*f2)*(τ5)+φ	[((-2π*f2)*(τ5)+φ)/π]*180			
2ω1-ω2	-0,51	(-2π*(2f1-f2))*(τ3)-φ	[((-2π*(2f1-f2))*(τ3)-φ)/π]*180	0,697	-0,25	-14,50
	1,22	(-2π*(2f1-f2))*(τ5)-φ	[((-2π*(2f1-f2))*(τ5)-φ)/π]*180			
2ω2-ω1	-0,54	(-2π*(2f2-f1))*(τ3)+2φ	[((-2π*(2f2-f1))*(τ3)+2φ)/π]*180	0,747	-0,48	-27,70
	1,26	(-2π*(2f2-f1))*(τ5)+2φ	[((-2π*(2f2-f1))*(τ5)+2φ)/π]*180			
3ω1-2ω2	0,24	(-2π*(3f1-2f2))*(τ5)-2φ	[((-2π*(3f1-2f2))*(τ5)-2φ)/π]*180	0,216	-0,33	-18,80
3ω2-2ω1	0,25	(-2π*(3f2-2f1))*(τ5)+3φ	[((-2π*(3f2-2f1))*(τ5)+3φ)/π]*180	0,279	-1,18	-67,70

Table A-15: Amplitude/Phase of Frequency Components of Measured Input Signal and Measured Output Signal When the Capacitor C3 is 30pF

16MHz - 30pF										
Input Signal				Output Signal						
Fundamentals				Fundamentals and Intermodulations						
	Frequency (MHz)	Amplitude (V)	Phase (°)		Frequency (MHz)	Amplitude (V)	Phase (°)			
f1	1492	4,7700	-55,4	f1	1492	18,6400	135,1			
f2	1508	4,9700	-54,3	f2	1508	19,2500	131,2			
				2f1-f2	1476	0,9441	-30,0			
				2f2-f1	1524	0,9831	-34,3	a5		
				3f1-2f2	1460	0,2474	-46,1	3f1-2f2	0,00015	Average
				3f2-2f1	1540	0,3008	-76,5	3f2-2f1	0,00017	0,00016

Table A-16: Amplitude/Phase of Frequency Components of Measured Output Signal When the Capacitor C3 is 30pF

16MHz-30pF						
Frequency	Amplitude (V)	Phase Expression (radian)	Phase Expression (°)	Amplitude (V)	Phase (radian)	Phase (°)
ω1	21,80	(-2π*f1)*(τ1)	-f1*(τ1)*360	18,640	2,36	135,10
	-1,52	(-2π*f1)*(τ3)	-f1*(τ3)*360			
	2,73	(-2π*f1)*(τ5)	-f1*(τ5)*360			
ω2	22,72	(-2π*f2)*(τ1)+φ	[((-2π*f2)*(τ1)+φ)/π]*180	19,250	2,29	131,20
	-1,54	(-2π*f2)*(τ3)+φ	[((-2π*f2)*(τ3)+φ)/π]*180			
	2,75	(-2π*f2)*(τ5)+φ	[((-2π*f2)*(τ5)+φ)/π]*180			
2ω1-ω2	-0,50	(-2π*(2f1-f2))*(τ3)-φ	[((-2π*(2f1-f2))*(τ3)-φ)/π]*180	0,944	-0,52	-30,00
	1,35	(-2π*(2f1-f2))*(τ5)-φ	[((-2π*(2f1-f2))*(τ5)-φ)/π]*180			
2ω2-ω1	-0,52	(-2π*(2f2-f1))*(τ3)+2φ	[((-2π*(2f2-f1))*(τ3)+2φ)/π]*180	0,983	-0,60	-34,30
	1,39	(-2π*(2f2-f1))*(τ5)+2φ	[((-2π*(2f2-f1))*(τ5)+2φ)/π]*180			
3ω1-2ω2	0,27	(-2π*(3f1-2f2))*(τ5)-2φ	[((-2π*(3f1-2f2))*(τ5)-2φ)/π]*180	0,247	-0,80	-46,10
3ω2-2ω1	0,28	(-2π*(3f2-2f1))*(τ5)+3φ	[((-2π*(3f2-2f1))*(τ5)+3φ)/π]*180	0,301	-1,33	-76,50

Table A-17: Amplitude/Phase of Frequency Components of Measured Input Signal and Measured Output Signal When the Capacitor C3 is 56pF

16MHz - 56pF										
Input Signal				Output Signal						
Fundamentals				Fundamentals and Intermodulations						
	Frequency (MHz)	Amplitude (V)	Phase (°)		Frequency (MHz)	Amplitude (V)	Phase (°)			
f1	1492	4,7600	-53,6	f1	1492	18,2800	133,6			
f2	1508	4,9100	-52,3	f2	1508	18,6900	129,9			
				2f1-f2	1476	1,1391	-32,8			
				2f2-f1	1524	1,1435	-38,5	a5		
				3f1-2f2	1460	0,2670	-53,1	3f1-2f2	0,00016	Average
				3f2-2f1	1540	0,3063	-80,1	3f2-2f1	0,00018	0,00017

Table A-18: Amplitude/Phase of Frequency Components of Measured Output Signal When the Capacitor C3 is 56pF

16MHz-56pF						
Frequency	Amplitude (V)	Phase Expression (radian)	Phase Expression (°)	Amplitude (V)	Phase (radian)	Phase (°)
ω1	21,76	(-2π*f1)*(τ1)	-f1*(τ1)*360	18,280	2,33	133,60
	-1,49	(-2π*f1)*(τ3)	-f1*(τ3)*360			
	2,80	(-2π*f1)*(τ5)	-f1*(τ5)*360			
ω2	22,44	(-2π*f2)*(τ1)+φ	[((-2π*f2)*(τ1)+φ)/π]*180	18,690	2,27	129,90
	-1,51	(-2π*f2)*(τ3)+φ	[((-2π*f2)*(τ3)+φ)/π]*180			
	2,82	(-2π*f2)*(τ5)+φ	[((-2π*f2)*(τ5)+φ)/π]*180			
2ω1-ω2	-0,49	(-2π*(2f1-f2))*(τ3)-φ	[((-2π*(2f1-f2))*(τ3)-φ)/π]*180	1,139	-0,57	-32,80
	1,39	(-2π*(2f1-f2))*(τ5)-φ	[((-2π*(2f1-f2))*(τ5)-φ)/π]*180			
2ω2-ω1	-0,51	(-2π*(2f2-f1))*(τ3)+2φ	[((-2π*(2f2-f1))*(τ3)+2φ)/π]*180	1,144	-0,67	-38,50
	1,42	(-2π*(2f2-f1))*(τ5)+2φ	[((-2π*(2f2-f1))*(τ5)+2φ)/π]*180			
3ω1-2ω2	0,28	(-2π*(3f1-2f2))*(τ5)-2φ	[((-2π*(3f1-2f2))*(τ5)-2φ)/π]*180	0,267	-0,93	-53,10
3ω2-2ω1	0,28	(-2π*(3f2-2f1))*(τ5)+3φ	[((-2π*(3f2-2f1))*(τ5)+3φ)/π]*180	0,306	-1,40	-80,10

Matlab scripts written can be seen below.

Script #1

```
clear all; close all; clc;


load 16mhzgiris.csv; % Time domain input signal captured with
oscilloscope

A = X16mhzgiris(:,1); % Time data
B = X16mhzgiris(:,2); % Voltage data
C = B*11.48; % Compensation of attenuation resulting from attenuator
D = C';

N = 25000; % Number of FFT

fs = 1.25*(10^10); % Sampling frequency

f = 0:fs/N:(fs/2)-(fs/N); % Frequency array

XapDFT1 = apfft(D, N);
% N-point all phase DFT coefficients. These coefficients have the
same
% properties as an N-point FFT does.
% Function uses a 2*N-1 point frame and returns N-point output.
% This function is written by Erdal Mehmetcik.

load 16mhzcikis.csv; % Time domain output signal captured with
oscilloscope
```

Script #1 continues

```
E = X16mhzcikis(:,1); % Time data
F = X16mhzcikis(:,2); % Voltage data
G = F*30.55; % Compensation of attenuation resulting from attenuator
H = G';

XapDFT2 = apfft(H, N); % FFT of time domain output signal


figure,
plot(E,G,'b')
hold on;
plot(E,C,'m') % Plot of time domain input and output signals

figure,
plot(f,abs(XapDFT1(1:end/2))/(N/2),'m')
% Plot of frequency spectrum of input signal
figure,
plot(f,abs(XapDFT2(1:end/2))/(N/2),'m')
% Plot of frequency spectrum of output signal

k=1;
for i=4:length(C)
    I(k) = (4.571*C(i-1,1))+(-0.0059*(C(i-2,1)^3))+(0.00011*(C(i-
3,1)^5));
    k=k+1;
end
% Simulated time domain output signal

XapDFT3 = apfft(I(1,1:49995),24998);
% FFT of simulated time domain output signal

K = I';

figure,
plot(E(4:49998),K(1:49995),'r')
hold on;
plot(E(4:49998),G(4:49998),'b')
% Plot of simulated time domain output signal and measured time
domain
% output signal

A4 = abs(XapDFT2(1:12499))/(N/2);
P4 = angle(XapDFT2(1:12499))*180/pi;
% Amplitude and Phase of Frequency Components of Measured Output
Signal

A5 = abs(XapDFT3(1:12499))/((N-2)/2);
P5 = angle(XapDFT3(1:12499))*180/pi;
% Amplitude and Phase of Frequency Components of Simulated Output
Signal

SUM1 = 0;
for l=1:49995
```

Script #1 continues

```
    SUM1 = SUM1 + (abs(A4(l)-A5(l))^2);
end

SUM2 = 0;
for l=1:49995
    SUM2 = SUM2 + (abs(A4(l))^2);
end



NMSE = 10*log10(SUM1/SUM2);
% Calculation of Normalized Mean Square Error

[pks, locs]= findpeaks(A4, 'minpeakheight', 18.90);
[pks2, locs2]= findpeaks(A4(locs(1)-
100:locs(2)+100),'minpeakheight', 0.187);
% Achieving amplitude and phase of each frequency components of
measured
% time domain output signal

disp('3f1-2f2:')
disp(f(locs(1)-101+locs2(1)))
disp('Amplitude of 3f1-2f2:')
disp(A4(locs(1)-101+locs2(1)))
disp('Phase of 3f1-2f2:')
disp(P4(locs(1)-101+locs2(1)))
% Amplitude and phase of frequency component 3f1-2f2

disp('2f1-f2:')
disp(f(locs(1)-101+locs2(2)))
disp('Amplitude of 2f1-f2:')
disp(A4(locs(1)-101+locs2(2)))
disp('Phase of 2f1-f2:')
disp(P4(locs(1)-101+locs2(2)))
% Amplitude and phase of frequency component 2f1-f2

disp('f1:')
disp(f(locs(1)-101+locs2(3)))
disp('Amplitude of f1:')
disp(A4(locs(1)-101+locs2(3)))
disp('Phase of f1:')
disp(P4(locs(1)-101+locs2(3)))
% Amplitude and phase of frequency component f1

disp('f2:')
disp(f(locs(1)-101+locs2(4)))
disp('Amplitude of f2:')
disp(A4(locs(1)-101+locs2(4)))
disp('Phase of f2:')
disp(P4(locs(1)-101+locs2(4)))
% Amplitude and phase of frequency component f2
```

Script #1 continues

```
disp('2f2-f1:')
disp(f(locs(1)-101+locs2(5)))
disp('Amplitude of 2f2-f1:')

disp(A4(locs(1)-101+locs2(5)))
disp('Phase of 2f2-f1:')
disp(P4(locs(1)-101+locs2(5)))
% Amplitude and phase of frequency component 2f2-f1

disp('3f2-2f1:')
disp(f(locs(1)-101+locs2(6)))
disp('Amplitude of 3f2-2f1:')
disp(A4(locs(1)-101+locs2(6)))


disp('Phase of 3f2-2f1:')
disp(P4(locs(1)-101+locs2(6)))
% Amplitude and phase of frequency component 3f2-2f1

[pks, locs]= findpeaks(A5, 'minpeakheight', 17.55);
[pks2, locs2]= findpeaks(A5(locs(1)-
100:locs(2)+100),'minpeakheight', 0.168);
% Achieving amplitude and phase of each frequency components of
simulated
% time domain output signal

disp('3f1-2f2:')
disp(f(locs(1)-101+locs2(1)))
disp('Amplitude of 3f1-2f2:')
disp(A5(locs(1)-101+locs2(1)))
disp('Phase of 3f1-2f2:')
disp(P5(locs(1)-101+locs2(1)))
% Amplitude and phase of frequency component 3f1-2f2

disp('2f1-f2:')
disp(f(locs(1)-101+locs2(2)))
disp('Amplitude of 2f1-f2:')
disp(A5(locs(1)-101+locs2(2)))
disp('Phase of 2f1-f2:')
disp(P5(locs(1)-101+locs2(2)))

disp('f1:')
disp(f(locs(1)-101+locs2(3)))
disp('Amplitude of f1:')
disp(A5(locs(1)-101+locs2(3)))
disp('Phase of f1:')
disp(P5(locs(1)-101+locs2(3)))

disp('f2:')
disp(f(locs(1)-101+locs2(4)))
disp('Amplitude of f2:')
disp(A5(locs(1)-101+locs2(4)))
```

Script #1 continues

```
disp('Phase of f2:')
disp(P5(locs(1)-101+locs2(4)))
disp('2f2-f1:')
disp(f(locs(1)-101+locs2(5)))
disp('Amplitude of 2f2-f1:')
disp(A5(locs(1)-101+locs2(5)))
disp('Phase of 2f2-f1:')
disp(P5(locs(1)-101+locs2(5)))


disp('3f2-2f1:')
disp(f(locs(1)-101+locs2(6)))
disp('Amplitude of 3f2-2f1:')
disp(A5(locs(1)-101+locs2(6)))
disp('Phase of 3f2-2f1:')
disp(P5(locs(1)-101+locs2(6)))
```

Script #2

```
function Fout = apfft(dat, NFFT)
% Fout = apfft(dat, NFFT)
%
% All phase fft, [1], implementation with reduced computational
load.
%
%
% dat : Time domain data of length => (2*NFFT-1)
% NFFT : DFT length
%
% [1] : "New method of estimation of phase, amplitude and frequency
based
%        on all-phase FFT spectrum analysis", Huang Xiaohong, Wang
Zhaohua,
%        Hou Guoqiang
%
%
% Erdal Mehmetcik

bufData = buffer(dat, 2*NFFT-1, NFFT-1, 'nodelay');
w1 = ones(1,NFFT);
w2 = ones(1,NFFT);

w = conv(w1, w2)/NFFT;

Fout = zeros(NFFT, size(bufData,2));
for k = 1 : size(bufData,2)
    datFrame = bufData(:, k).*w';
    xData = [datFrame(NFFT) ; (datFrame(1:NFFT-1)+datFrame(NFFT+1 :
2*NFFT-1))];
    Fout(:, k) = fft(xData, NFFT);
end
```

Script #2 is written by Erdal Mehmetcik to achieve amplitude and exact phase of frequency components.

Script #3

```
clear all; close all; clc;


v1 = 4.76; % Amplitude of frequency component f1 of input signal
v2 = 4.91; % Amplitude of frequency component f2 of input signal

x1 = 0.267; % Amplitude of frequency component 3f1-2f2 of output
signal
x2 = 0.306; % Amplitude of frequency component 3f2-2f1 of output
signal

a51 = x1/(5/8*(v1^3)*(v2^2));
a51 = roundn(a51,-5);
% Calculation of a5 coefficient from amplitude expression of 3f1-2f2
a52 = x2/(5/8*(v1^2)*(v2^3));

a52 = roundn(a52,-5);
% Calculation of a5 coefficient from amplitude expression of 3f2-2f1
```

Script #4

```
clear all; close all; clc;


V1 = 4.76; % Amplitude of frequency component f1 of input signal
V2 = 4.91; % Amplitude of frequency component f2 of input signal

a1 = 4.571; % Coefficient a1
a3 = -0.0059; % Coefficient a3
a5 = 0.00017; % Coefficient a5

A = a1*V1;
A1 = roundn(A,-2);
% Amplitude of first term of frequency component f1 of output signal

B = (3/4*a3*(V1^3))+(3/2*a3*V1*(V2^2));
B1 = roundn(B,-2);
% Amplitude of second term of frequency component f1 of output
signal

C = (5/8*a5*(V1^5))+(15/4*a5*(V1^3)*(V2^2))+(15/8*a5*V1*(V2^4));
C1 = roundn(C,-2);
% Amplitude of third term of frequency component f1 of output signal
 D = a1*V2;
```

Script #4 continues

```
D1 = roundn(D,-2);
% Amplitude of first term of frequency component f2 of output signal

E = (3/4*a3*(V2^3))+(3/2*a3*V2*(V1^2));
E1 = roundn(E,-2);
% Amplitude of second term of frequency component f2 of output
signal

F = (5/8*a5*(V2^5))+(15/4*a5*(V1^2)*(V2^3))+(15/8*a5*V2*(V1^4));
F1 = roundn(F,-2);
% Amplitude of third term of frequency component f2 of output signal

K = (3/4*a3*(V1^2)*V2);
K1 = roundn(K,-2);
% Amplitude of first term of frequency component 2f1-f2 of output
signal

L = (5/4*a5*(V1^4)*V2)+(15/8*a5*(V1^2)*(V2^3));
L1 = roundn(L,-2);
% Amplitude of second term of frequency component 2f1-f2 of output
signal
M = (3/4*a3*(V2^2)*V1);
M1 = roundn(M,-2);
% Amplitude of first term of frequency component 2f2-f1 of output
signal

N = (5/4*a5*(V2^4)*V1)+(15/8*a5*(V1^3)*(V2^2));
N1 = roundn(N,-2);
% Amplitude of second term of frequency component 2f2-f1 of output
signal

O = (5/8*a5*(V1^3)*(V2^2));
O1 = roundn(O,-2);
% Amplitude of frequency component 3f1-2f2 of output signal

P = (5/8*a5*(V1^2)*(V2^3));
P1 = roundn(P,-2);
% Amplitude of frequency component 3f2-2f1 of output signal
```